# The role of the GGOS network in the definition of high precision geodynamic parameters

Giuseppe Bianco[1] and Cinzia Luceri[2]

[1]Head, Space Research Dept., Italian Space Agency

[2]Head, Matera Space Center, e-Geos S.p.A.

IV International Workshop on Gravitomagnetism and Large-Scale RotationMeasurement

Pisa, Italy, 14-16 June 2023

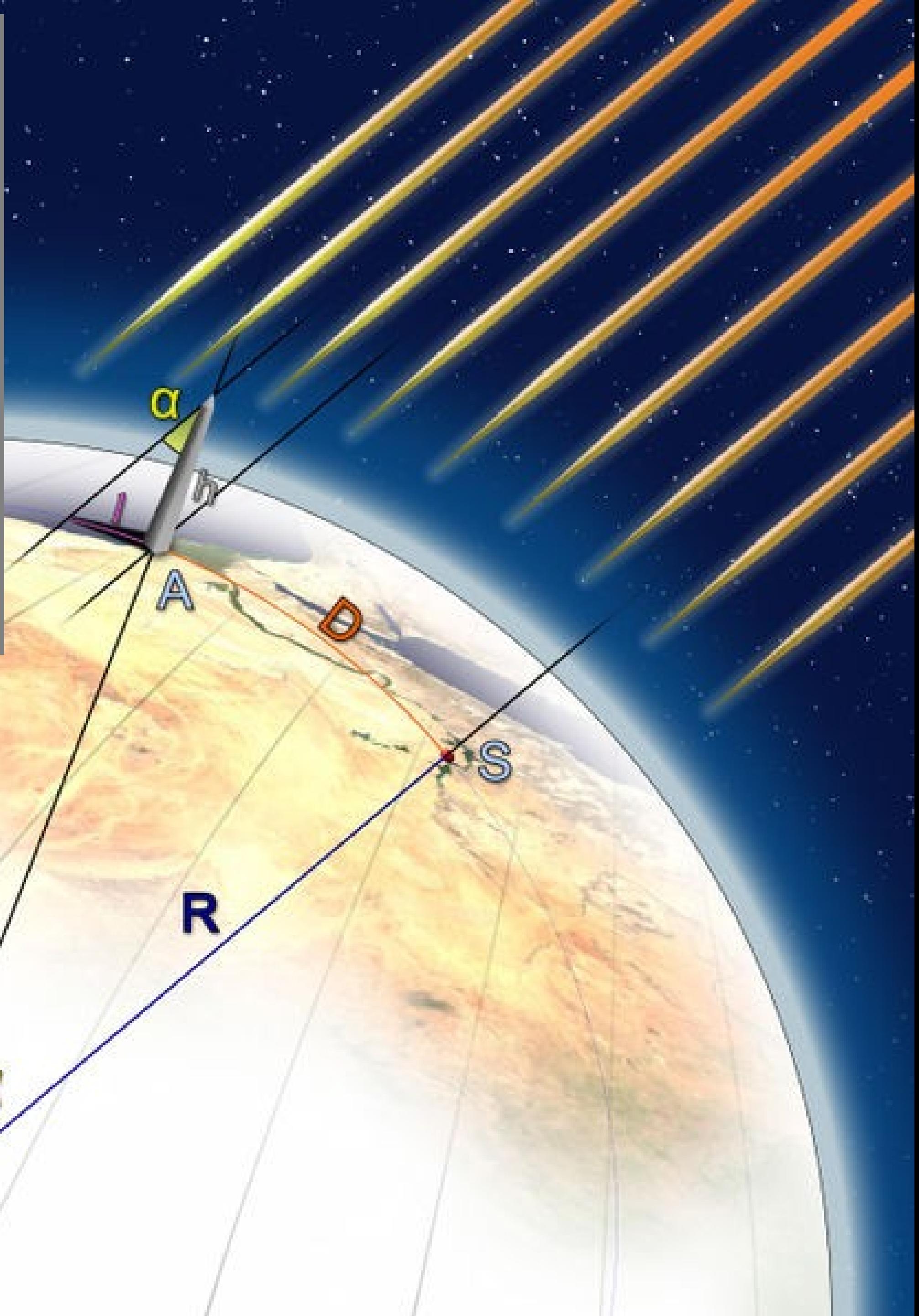
α
h
A
D
S
R
α

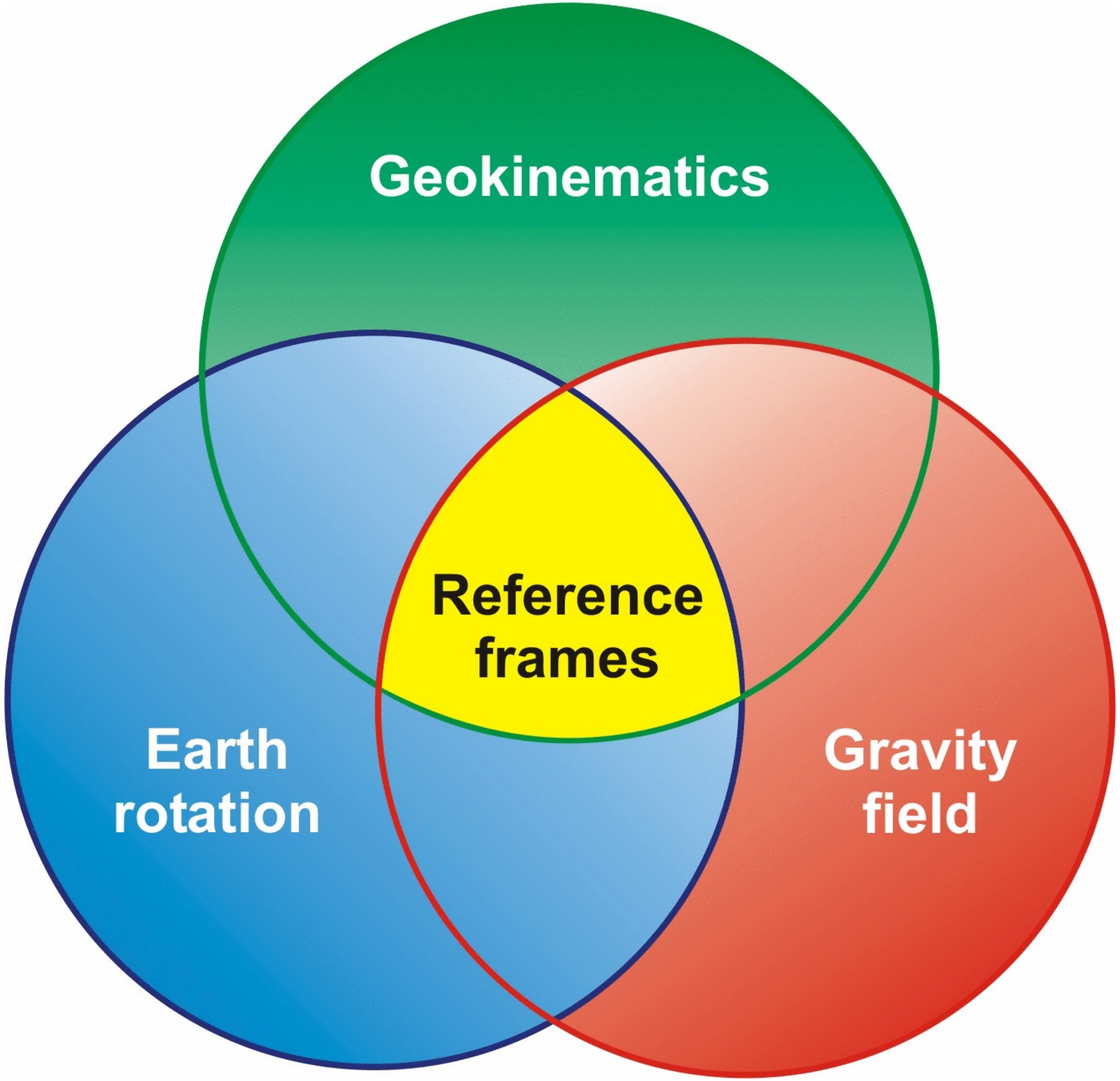
Geokinematics
Reference frames
Earth rotation
Gravity field

# Global Geodetic Observing System

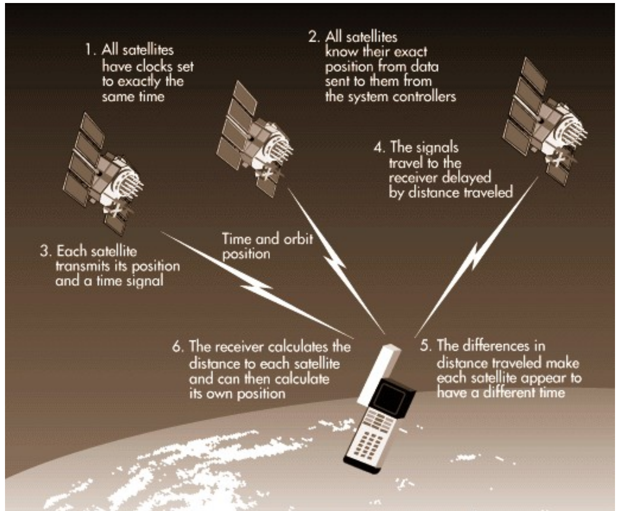

# GGOS

Global Geodetic Observing System

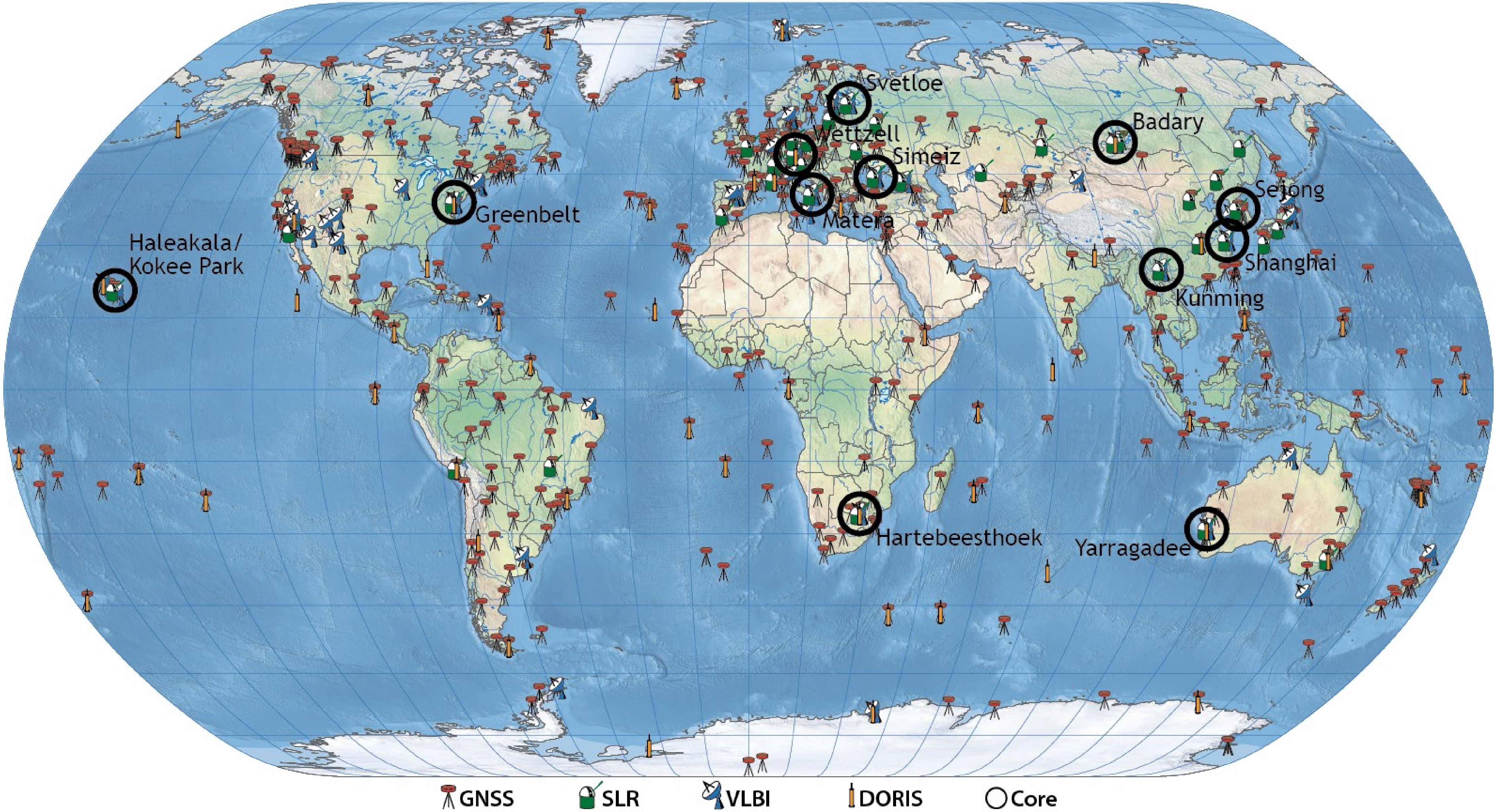

# Satellite Laser Ranging (SLR)

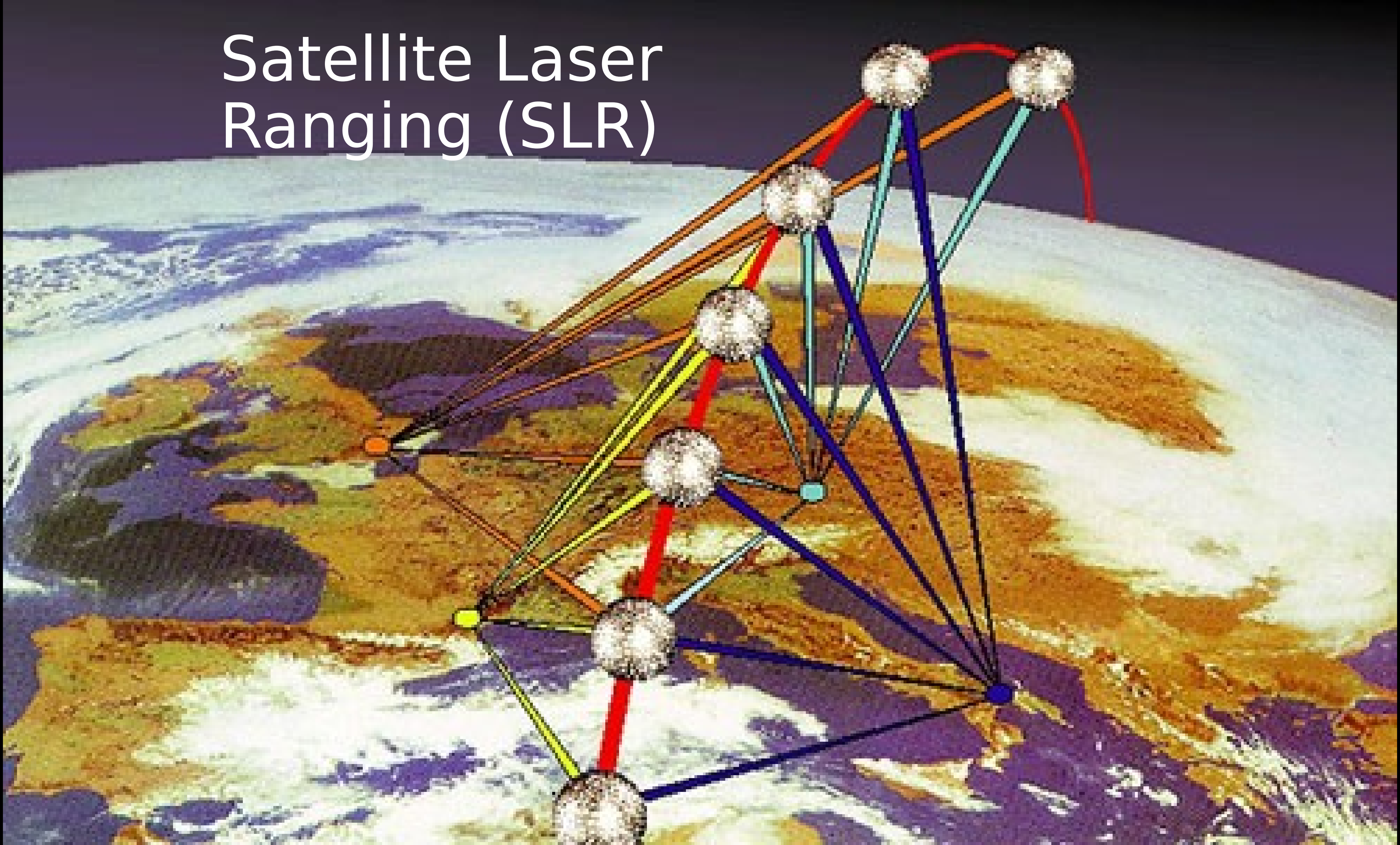

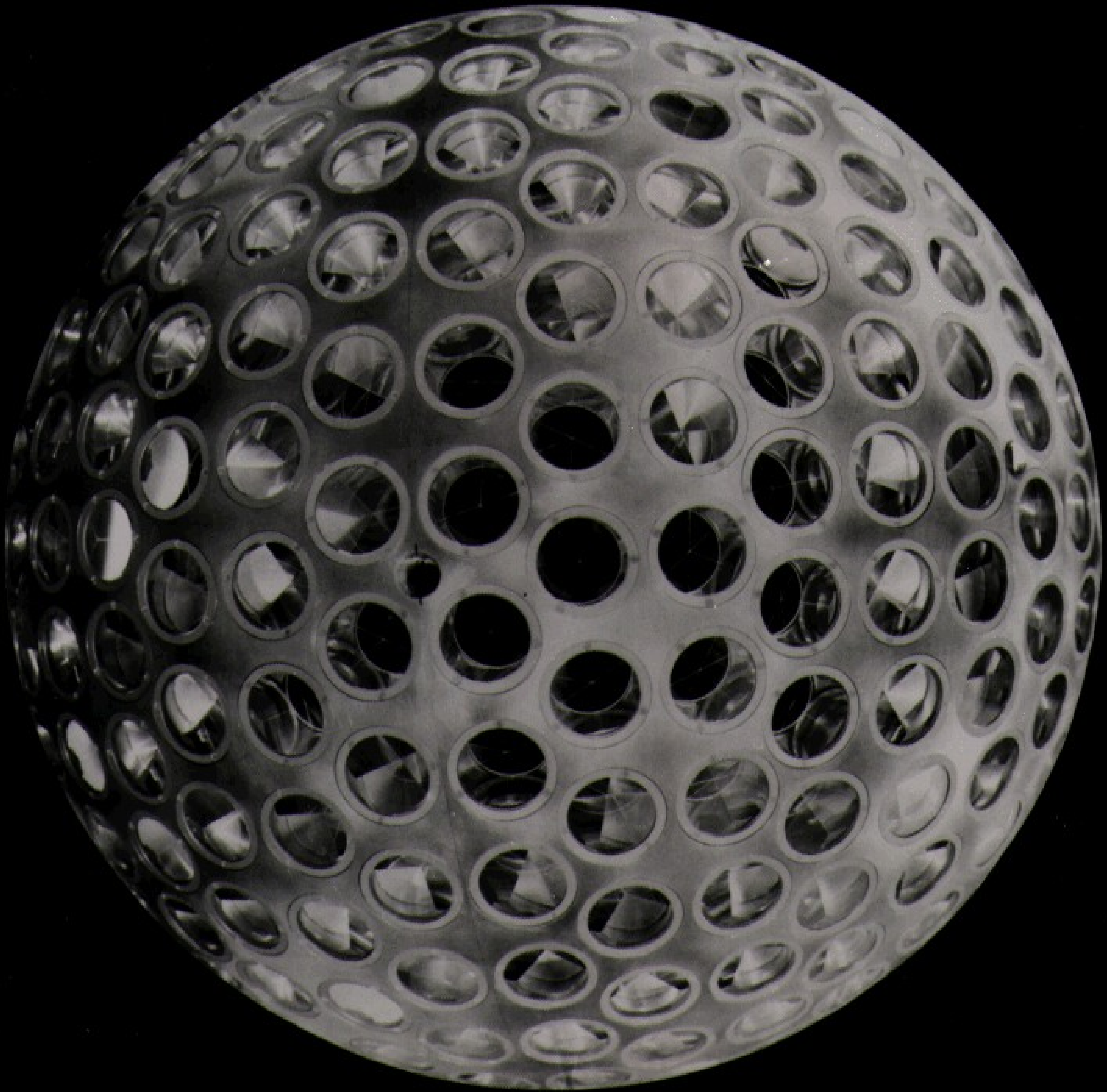

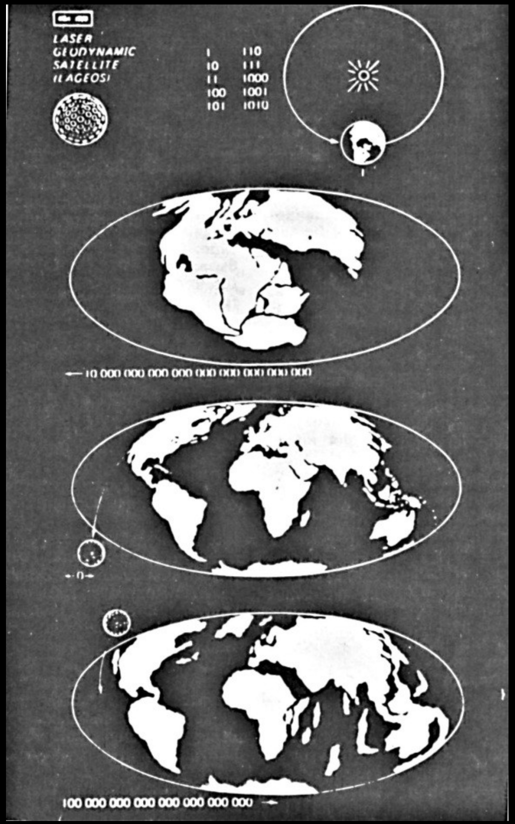
LASER
GEODYNAMIC
SATELLITE
(LAGEOS)
1 110
10 111
11 1000
100 1001
101 1010
10 000 000 000 000 000 000 000 000 000
100 000 000 000 000 000 000 000 000

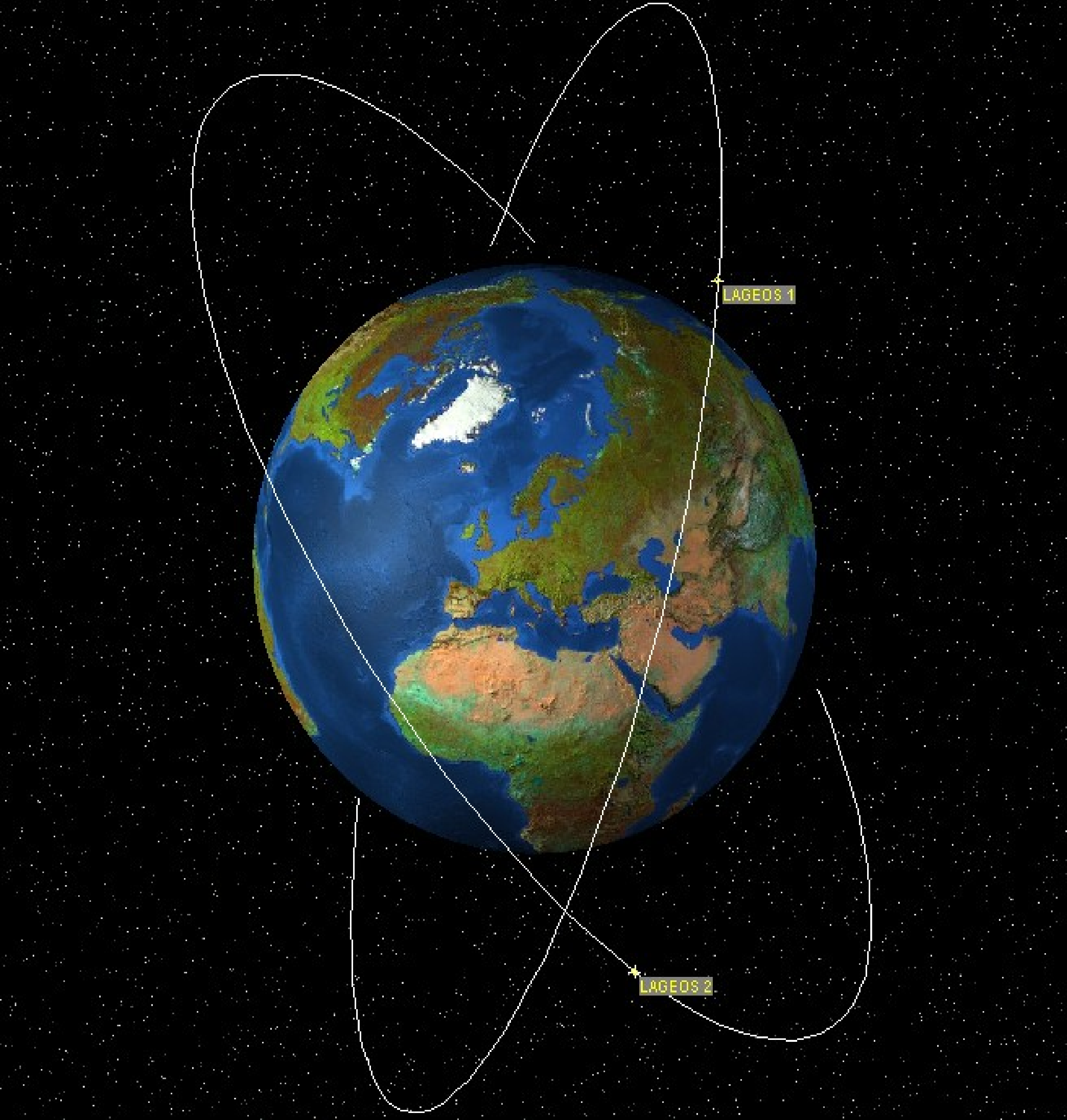
LAGEOS 1
LAGEOS 2

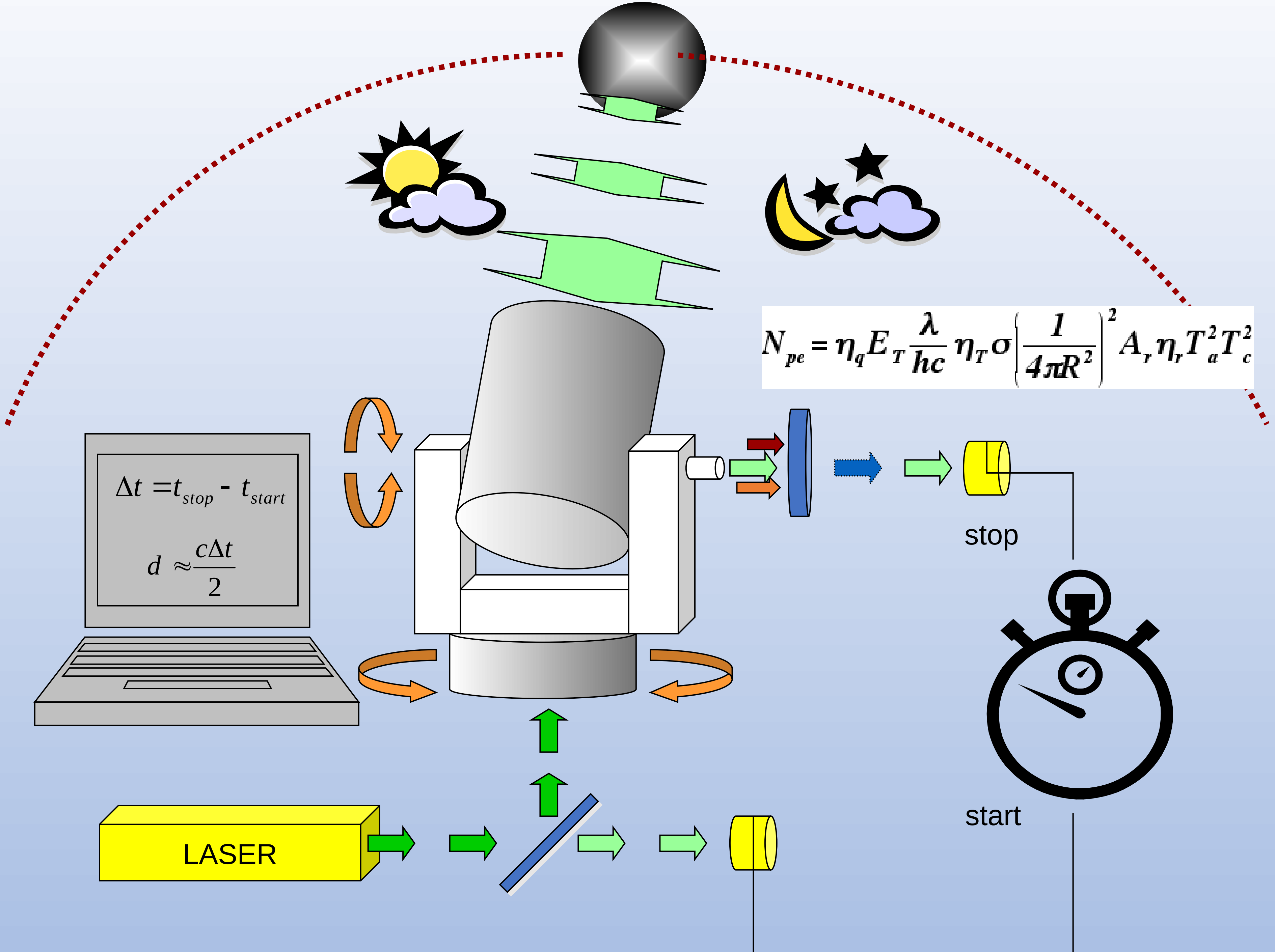

$N_{pe} = \eta_q E_T \frac{\lambda}{hc} \eta_T \sigma \left( \frac{1}{4\pi R^2} \right)^2 A_r \eta_r T_a^2 T_c^2$
$\Delta t = t_{stop} - t_{start}$
$d \approx \frac{c\Delta t}{2}$
stop
start
LASER


MLRO

# Very Long Baseline Interferometry (VLBI)

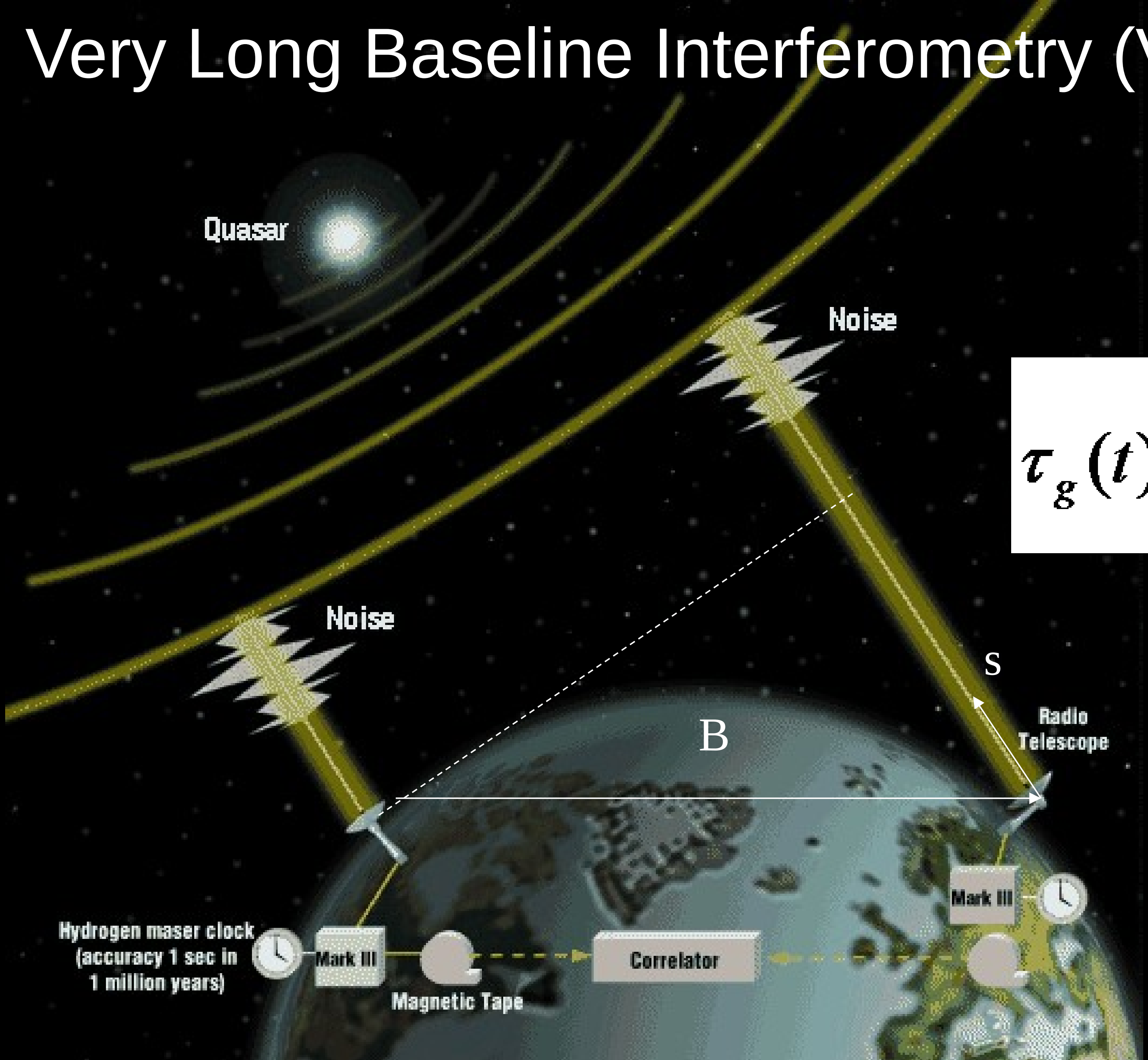


$$\tau_g(t) = \frac{\vec{B} \bullet \vec{s}}{c}$$

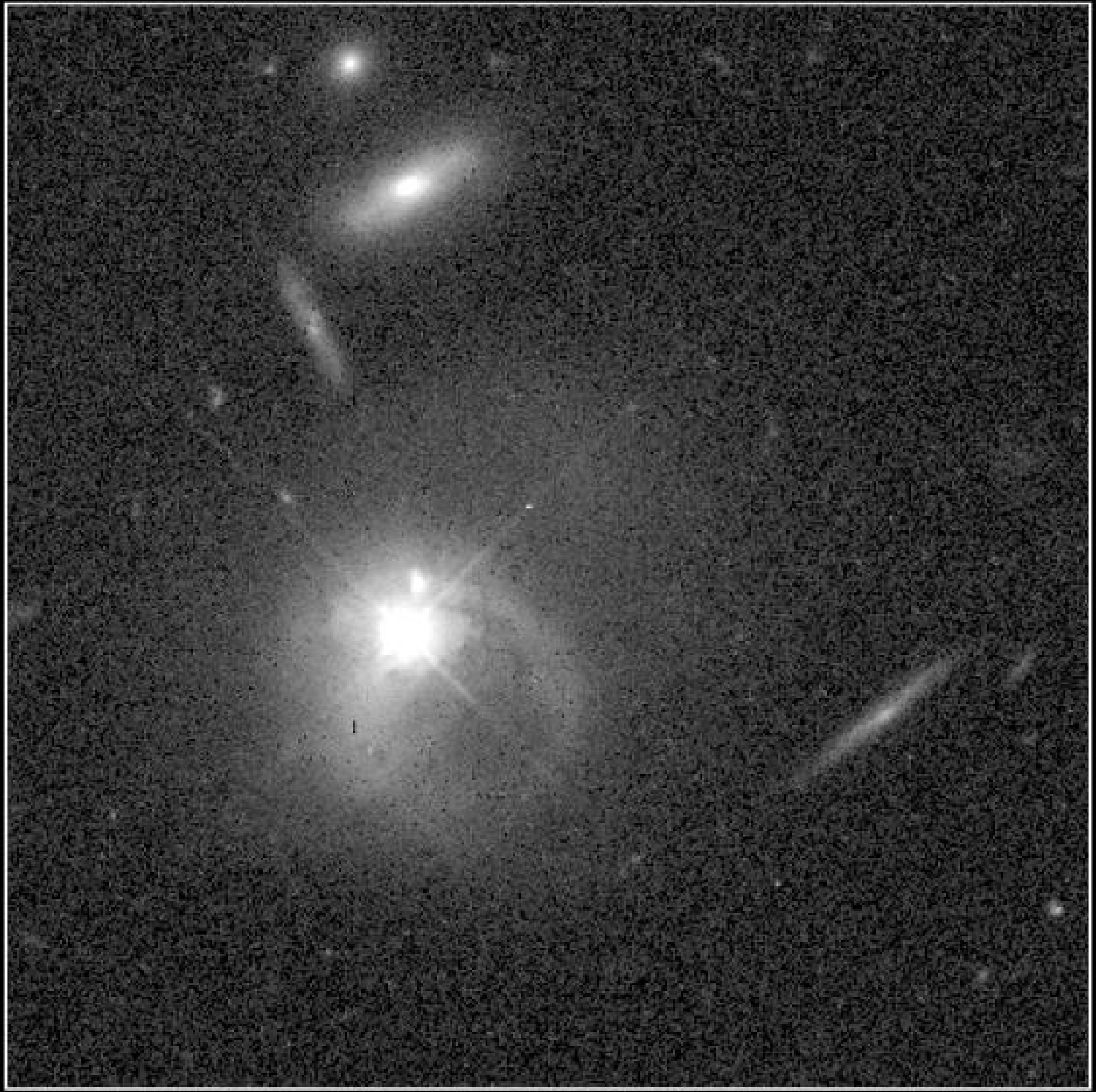

**Quasar PKS 2349** HST • WFPC2

ST ScI OPO • January 1995 • J. Bahcall (Princeton), NASA

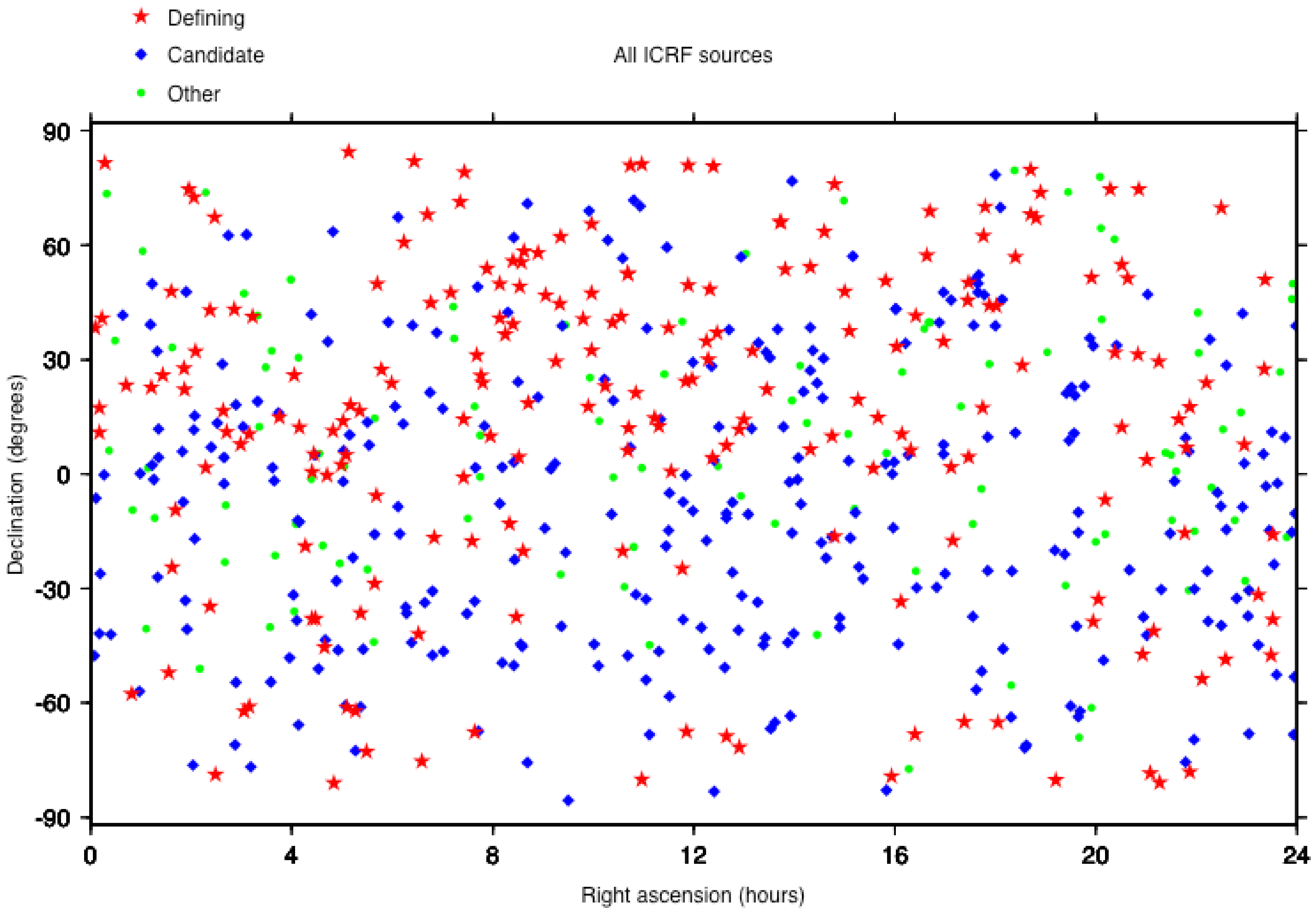
Defining
Candidate
Other
All ICRF sources
Declination (degrees)
90
60
30
0
-30
-60
-90
0
4
8
12
16
20
24
Right ascension (hours)

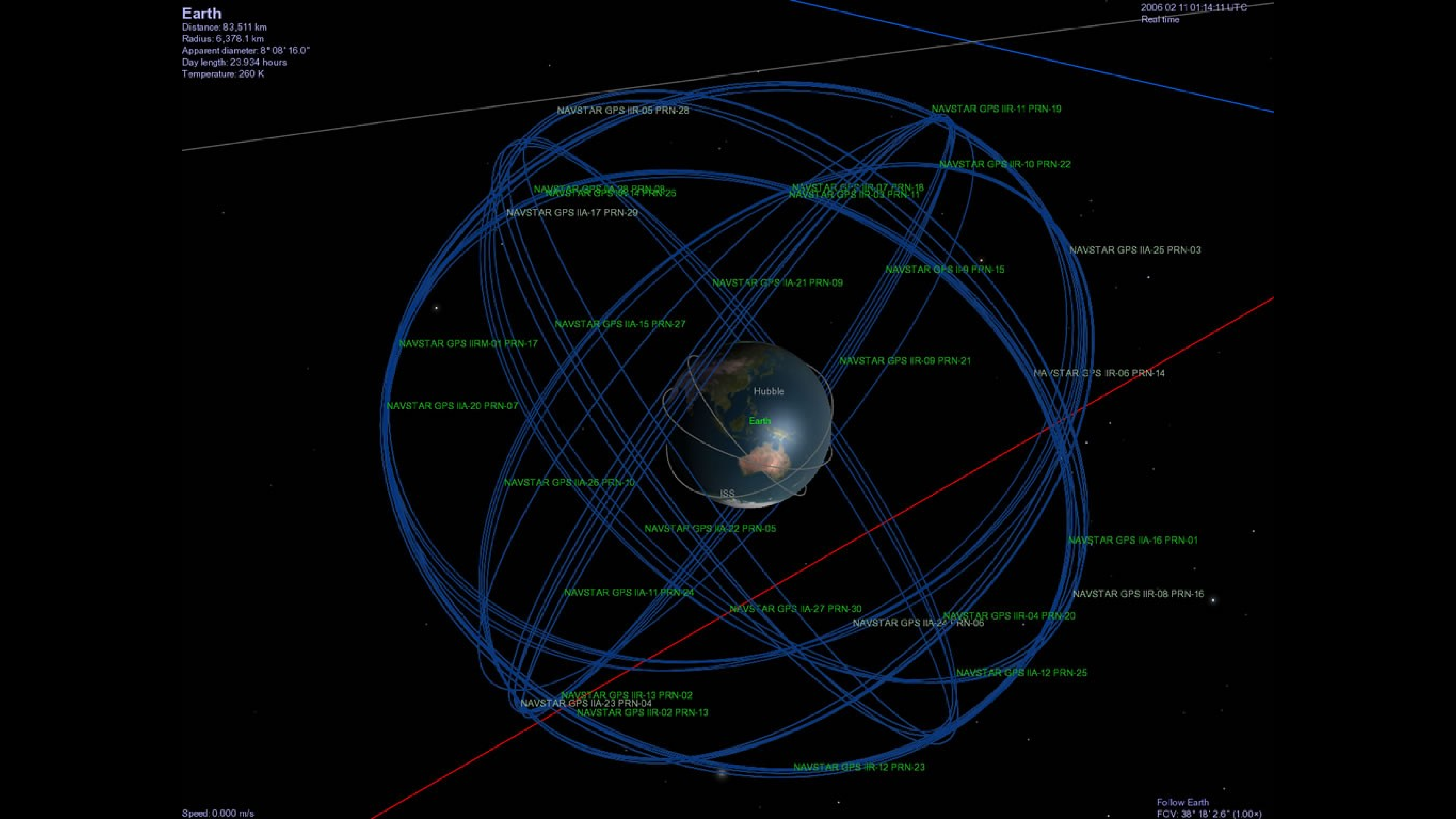

Earth
Distance: 83,511 km
Radius: 6,378.1 km
Apparent diameter: 8° 08' 16.0"
Day length: 23.934 hours
Temperature: 260 K
2006 02 11 01:14:11 UTC
Real time
NAVSTAR GPS IIR-05 PRN-28
NAVSTAR GPS IIR-11 PRN-19
NAVSTAR GPS IIR-10 PRN-22
NAVSTAR GPS IIA-17 PRN-29
NAVSTAR GPS IIA-25 PRN-03
NAVSTAR GPS II-9 PRN-15
NAVSTAR GPS IIA-21 PRN-09
NAVSTAR GPS IIA-15 PRN-27
NAVSTAR GPS IIRM-01 PRN-17
NAVSTAR GPS IIR-09 PRN-21
NAVSTAR GPS IIR-06 PRN-14
Hubble
NAVSTAR GPS IIA-20 PRN-07
Earth
NAVSTAR GPS IIA-26 PRN-10
ISS
NAVSTAR GPS IIA-22 PRN-05
NAVSTAR GPS IIA-16 PRN-01
NAVSTAR GPS IIA-11 PRN-24
NAVSTAR GPS IIR-08 PRN-16
NAVSTAR GPS IIA-27 PRN-30
NAVSTAR GPS IIR-04 PRN-20
NAVSTAR GPS IIA-24 PRN-06
NAVSTAR GPS IIA-12 PRN-25
NAVSTAR GPS IIR-13 PRN-02
NAVSTAR GPS IIA-23 PRN-04
NAVSTAR GPS IIR-02 PRN-13
NAVSTAR GPS IIR-12 PRN-23
Speed: 0.000 m/s
Follow Earth
FOV: 38° 18' 2.6" (1.00×)

## Global Navigation Satellite System

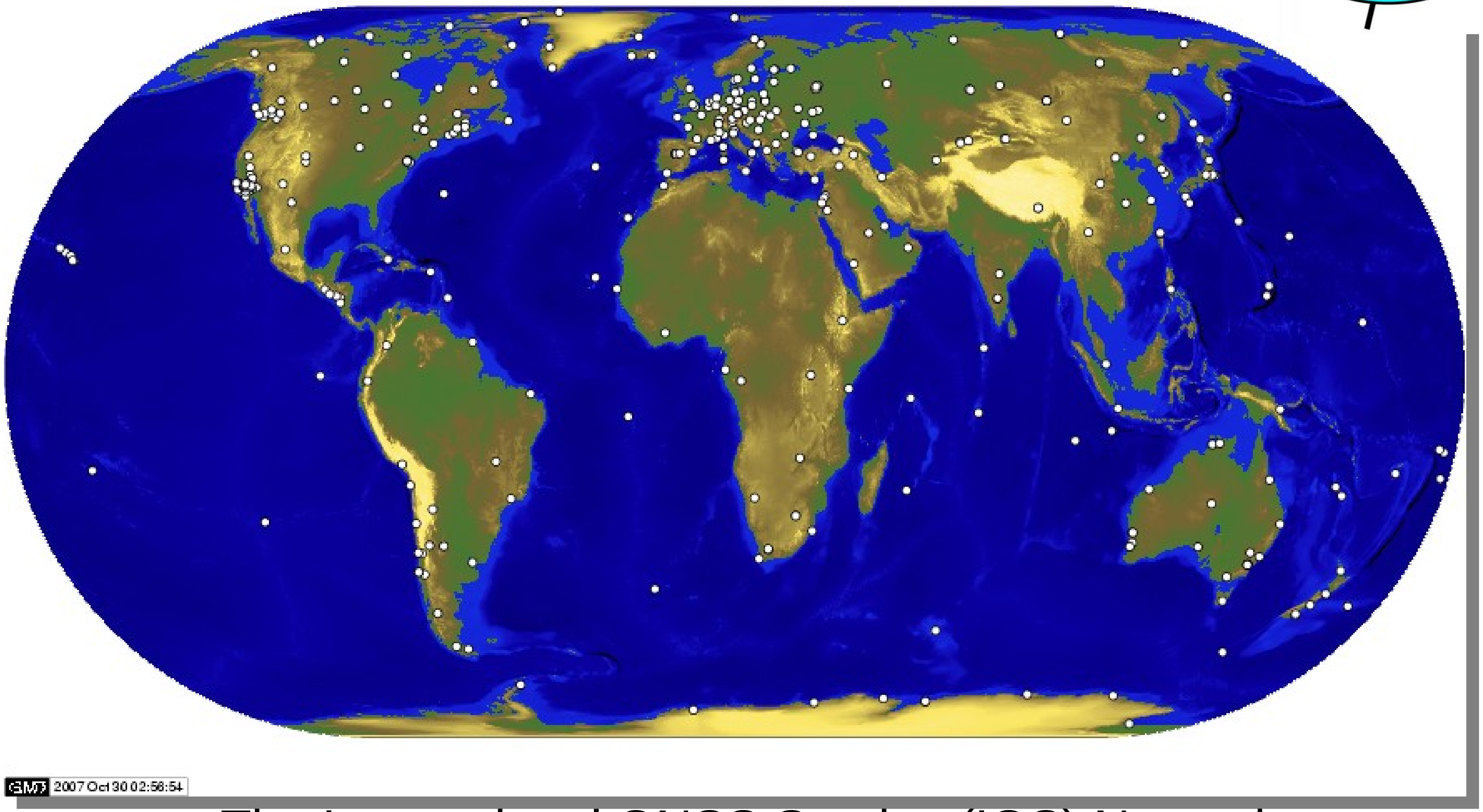


The International GNSS Service (IGS) Network

# Rete Fiduciale GNSS dell'ASI

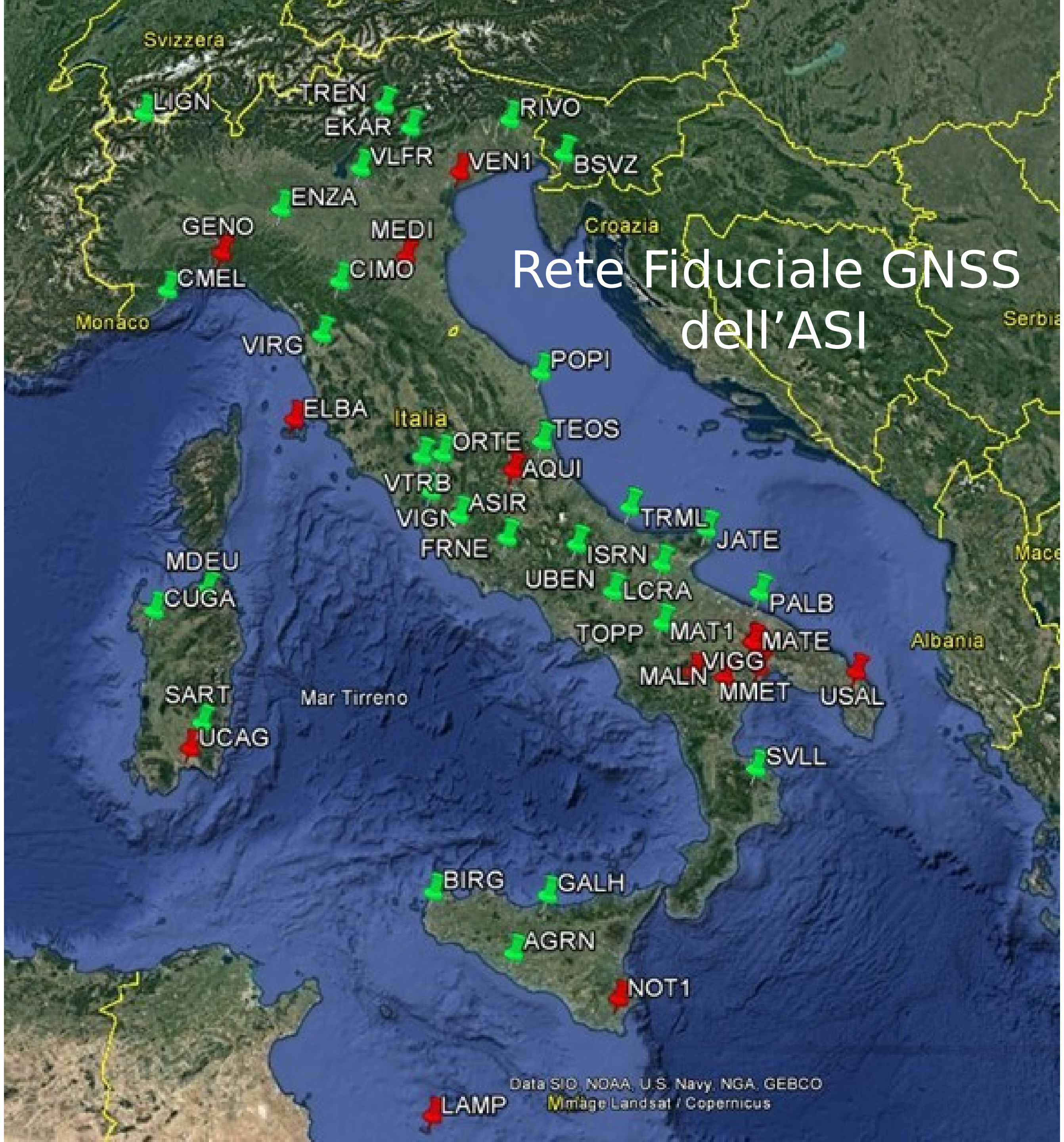

# ITRF2020: Preliminary horizontal velocity field

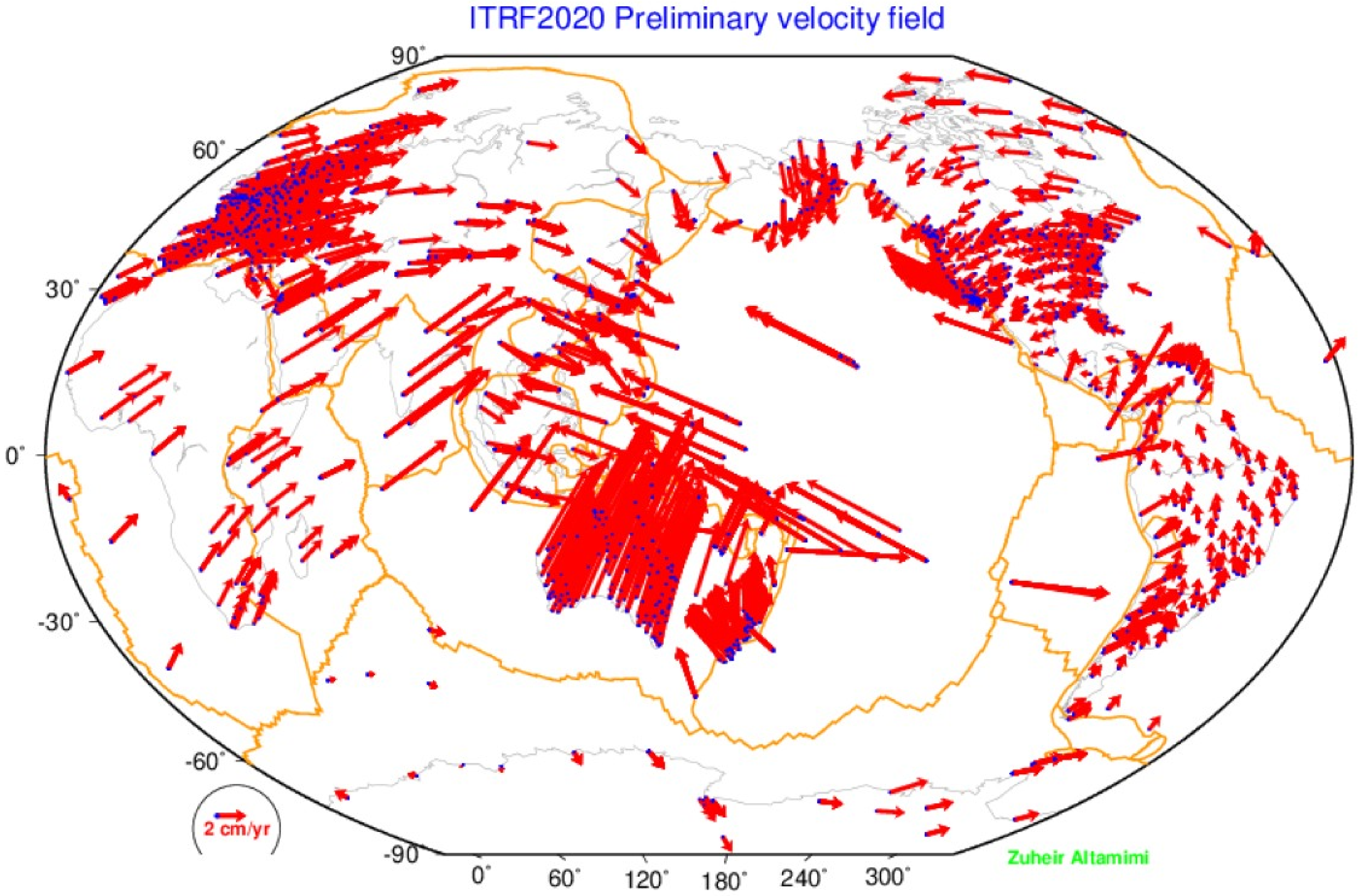

## Mean sea level change

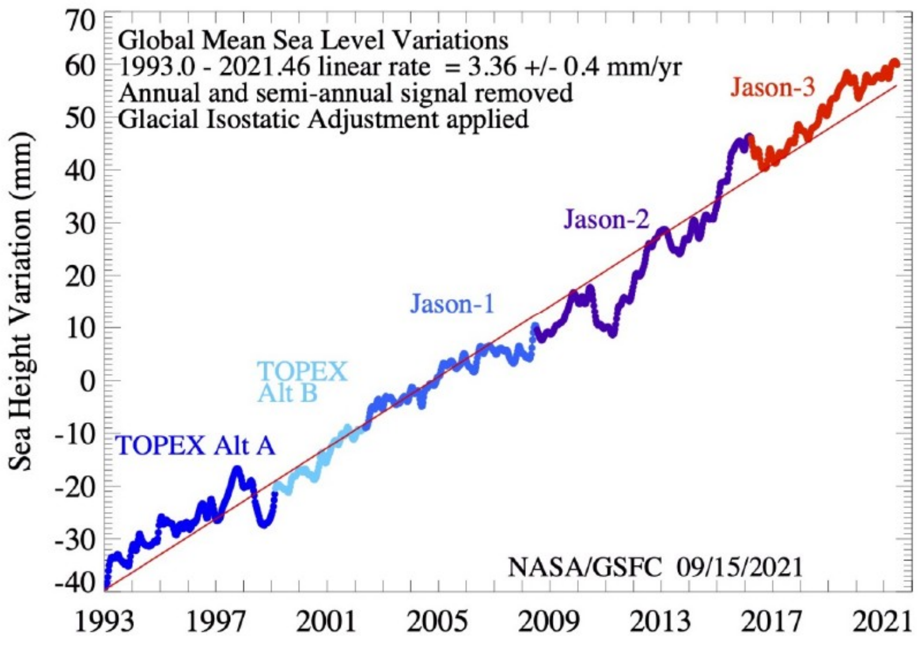


## ITRF2020: Preliminary vertical velocity field

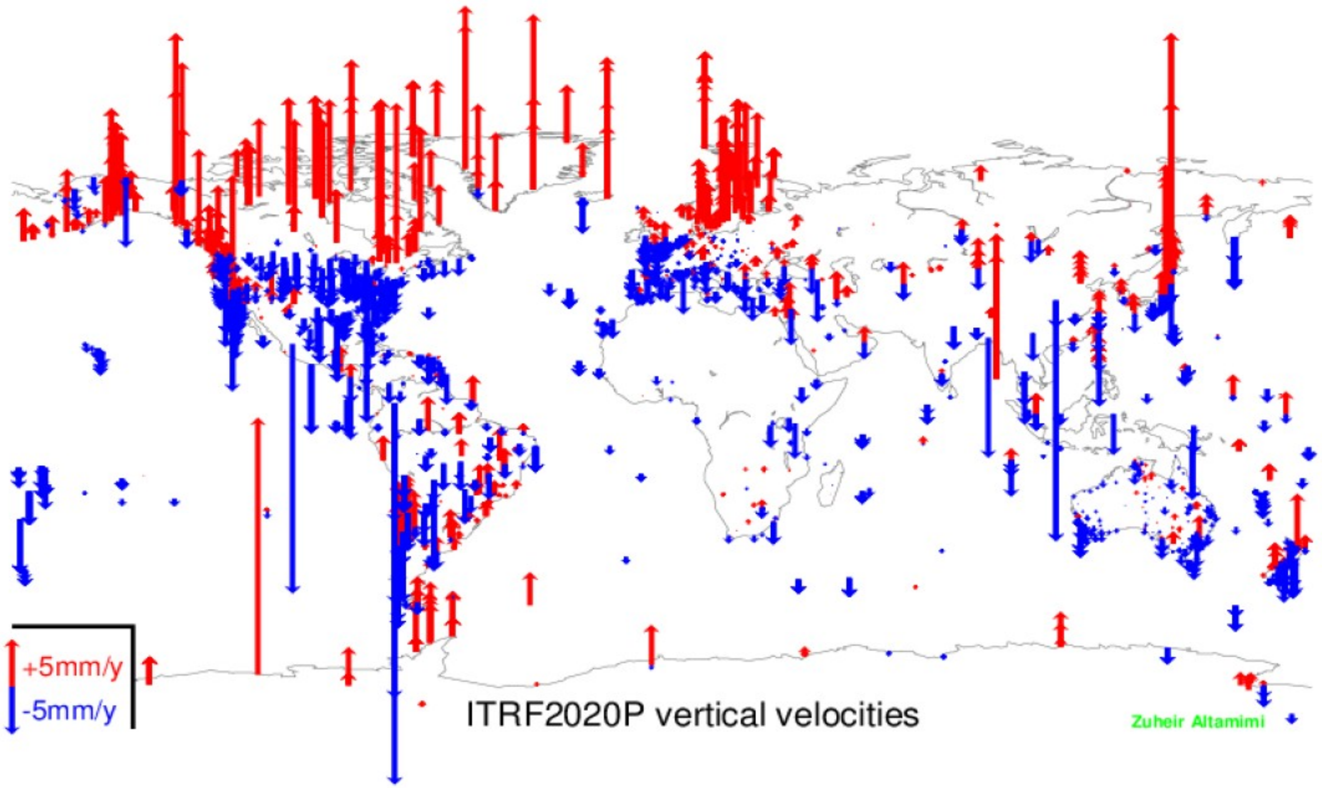

**Table 1 | Main 2007 tests of the general theory of relativity**

| Phenomenon or principle tested | Method and 2007 experimental limit |
|---|---|
| Weak equivalence principle (test-particles fall with the same acceleration; this is at the foundations of geometrical (metric) theories of gravitation) | Laboratory experiments (accuracy of the order of $10^{-13}$)<br>Lunar laser ranging (accuracy of the order of $10^{-13}$) |
| Strong equivalence principle (this is at the foundations of the general theory of relativity) | Lunar laser ranging (accuracy of less than $10^{-3}$) |
| Gravitational time dilation or gravitational redshift (relative slowing down of clocks near a mass) | Gravity Probe A (with a clock on the ground and one on a rocket; accuracy of the order of $10^{-4}$) |
| Deflection of photons' path and travel time-delay of electromagnetic waves, or Shapiro time-delay, by a mass | VLBI (accuracy of the order of $2\times 10^{-4}$)<br>Cassini spacecraft tracking (accuracy of the order of $10^{-5}$) |
| Perihelion advance of Mercury | Mercury radar ranging (accuracy of the order of $10^{-3}$) |
| Periastron advance, time dilation, time delay, rate of change of the orbital period (accurately explained by the loss of energy due to the emission of gravitational waves from a binary system) and other relativistic parameters (these effects are characterized by strong gravitational field inside a pulsar) | Binary pulsar PSR1913+16<br>Other binary pulsars |
| Lense–Thirring effect, or frame-dragging of a gyroscope by the spin of a body | LAGEOS and LAGEOS2 laser ranging (accuracy of the order of $10^{-1}$)<br>Gravity Probe B (it might be detected by further GP-B data analysis) |
| Geodetic precession, or de Sitter effect (dragging of a gyroscope due to its motion in a static gravitational field) | Lunar laser ranging (accuracy of the order of $6\times 10^{-3}$)<br>Gravity Probe B (accuracy of the order of $1.5\times 10^{-2}$; it should be improved by further Gravity Probe B data analysis)<br>Binary pulsars |

For a detailed description see refs 7, 8 and 3; for an update see ref. 9.

# LUNAR LASER RANGING

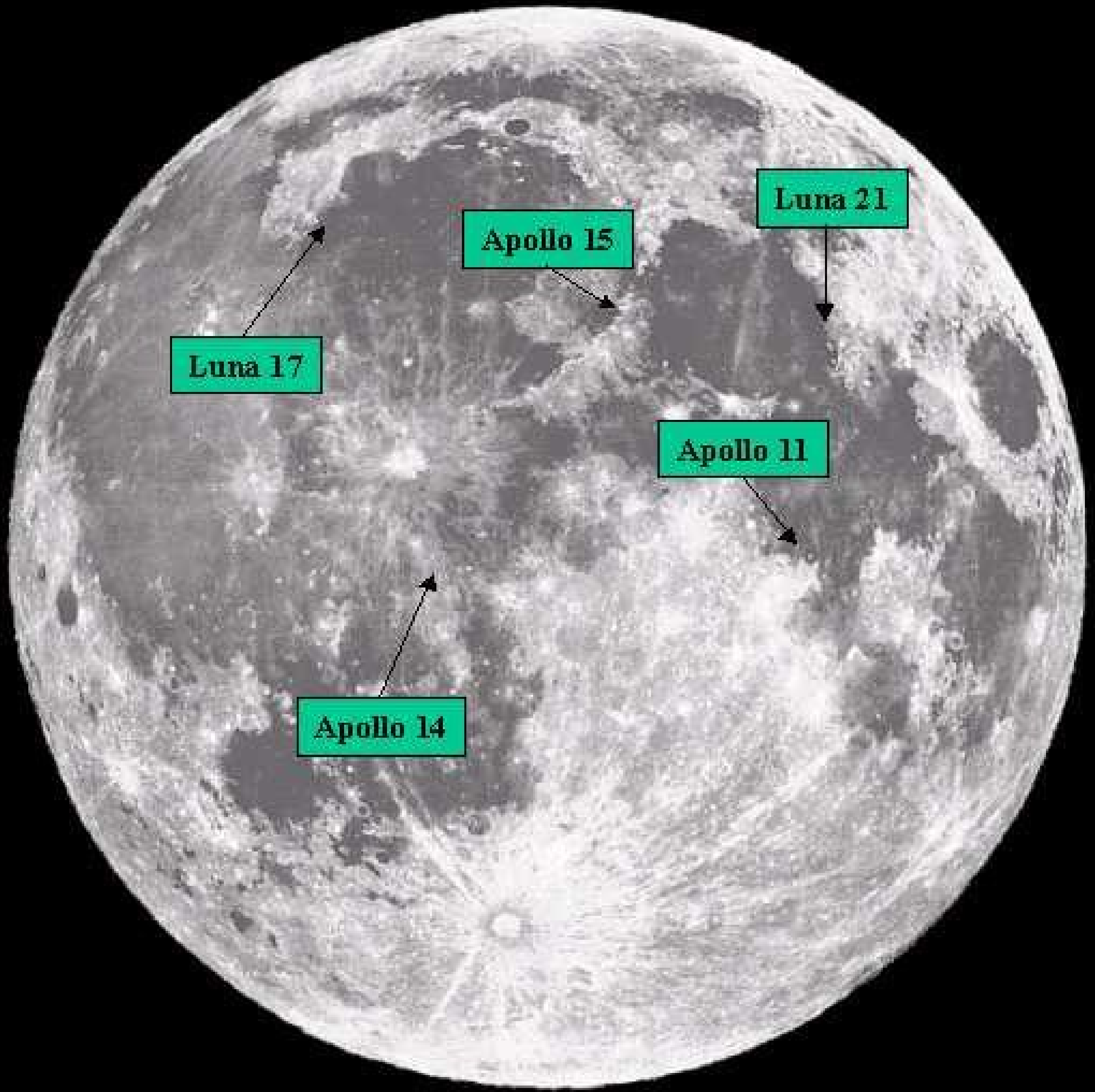

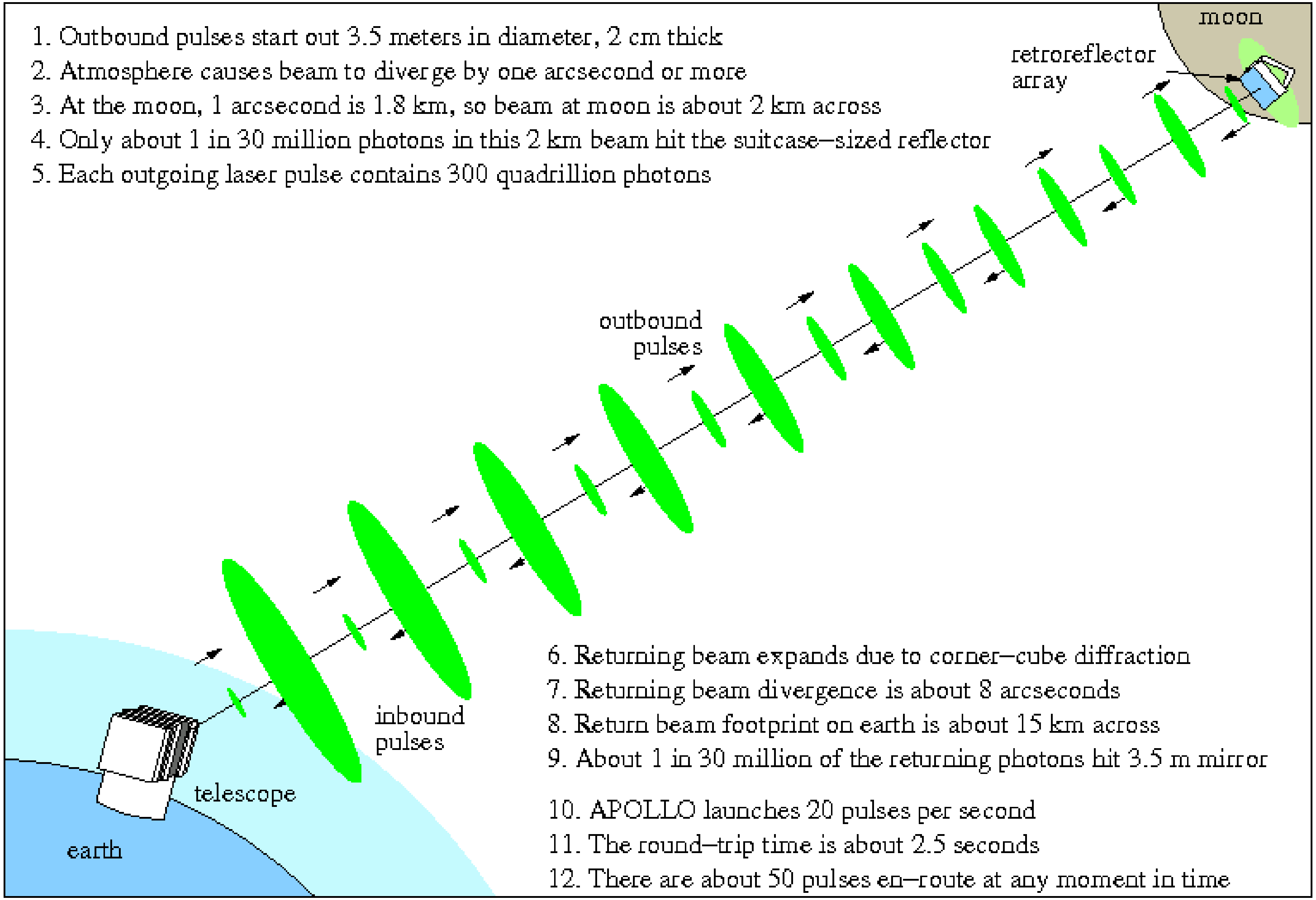
1. Outbound pulses start out 3.5 meters in diameter, 2 cm thick
2. Atmosphere causes beam to diverge by one arcsecond or more
3. At the moon, 1 arcsecond is 1.8 km, so beam at moon is about 2 km across
4. Only about 1 in 30 million photons in this 2 km beam hit the suitcase–sized reflector
5. Each outgoing laser pulse contains 300 quadrillion photons
moon
retroreflector array
outbound pulses
inbound pulses
telescope
earth
6. Returning beam expands due to corner–cube diffraction
7. Returning beam divergence is about 8 arcseconds
8. Return beam footprint on earth is about 15 km across
9. About 1 in 30 million of the returning photons hit 3.5 m mirror
10. APOLLO launches 20 pulses per second
11. The round–trip time is about 2.5 seconds
12. There are about 50 pulses en–route at any moment in time

# Gravitomagnetic field (Lense-Thirring effect)

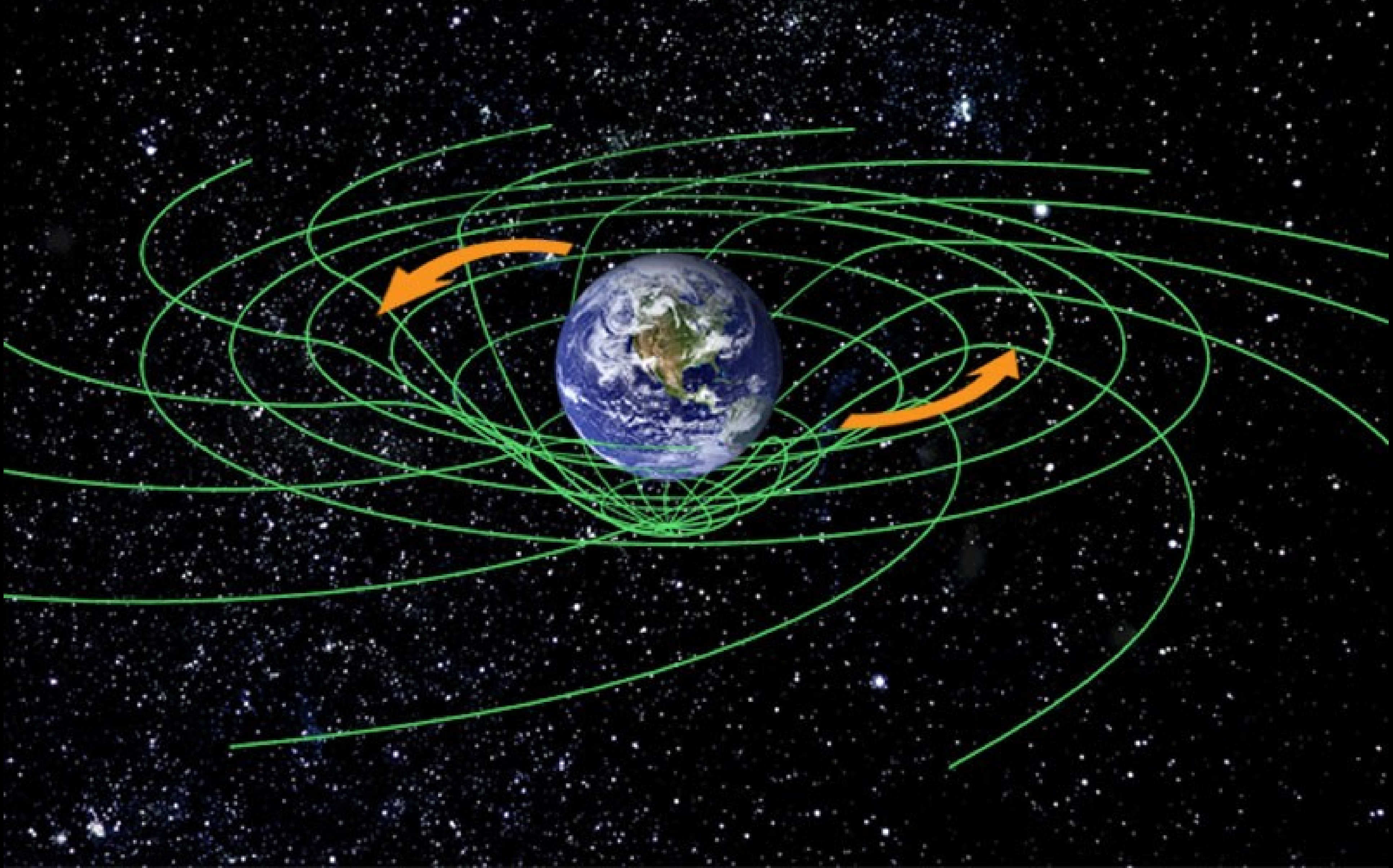

# LARES-2 (Laser Relativity Satellite 2)

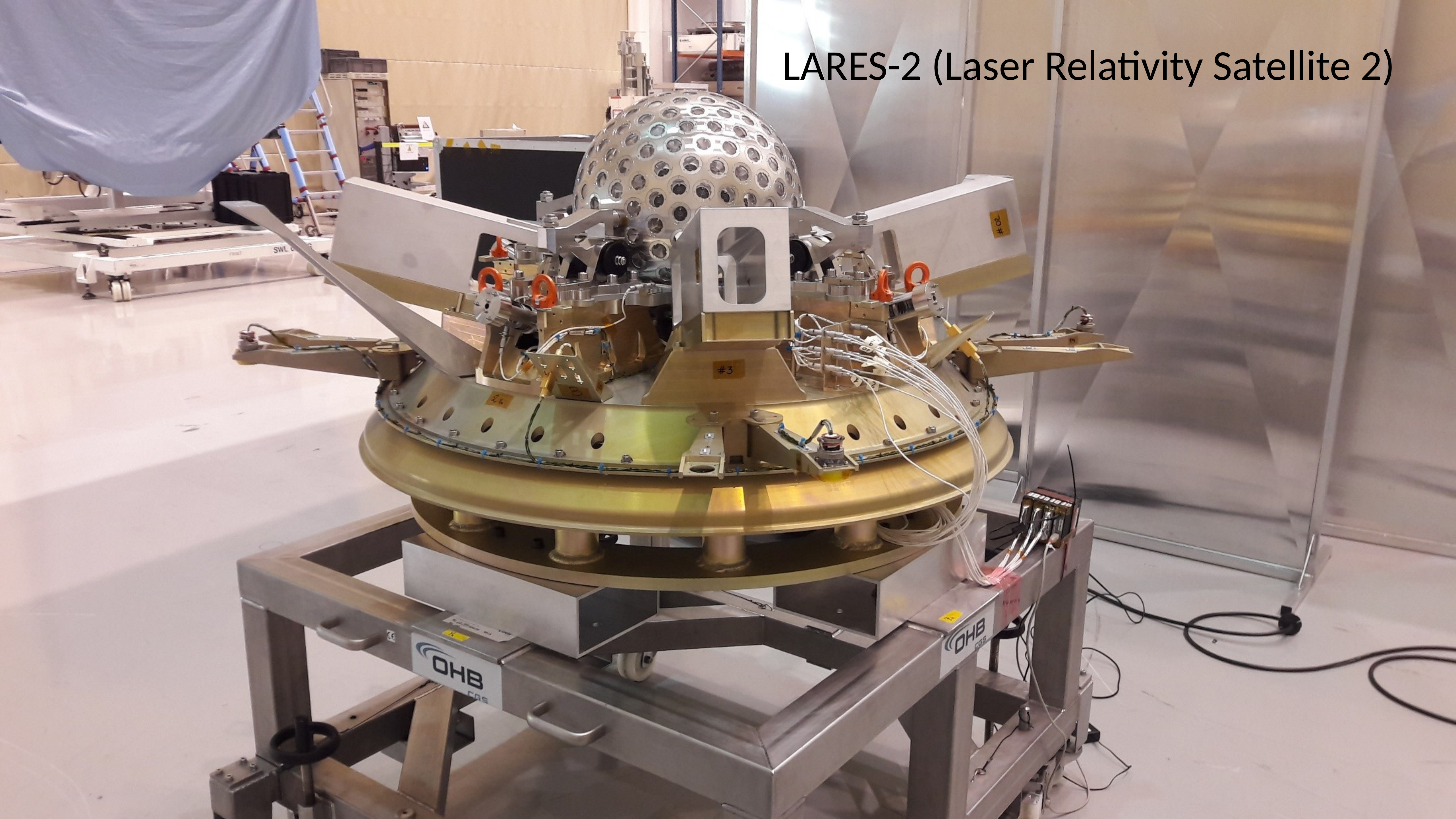

# Metrology: the Italian Link for Frequency & Time (LIFT)

ISTITUTO NAZIONALE DI RICERCA METROLOGICA

## Turin

## Florence

INO-CNR ISTITUTO NAZIONALE DI OTTICA

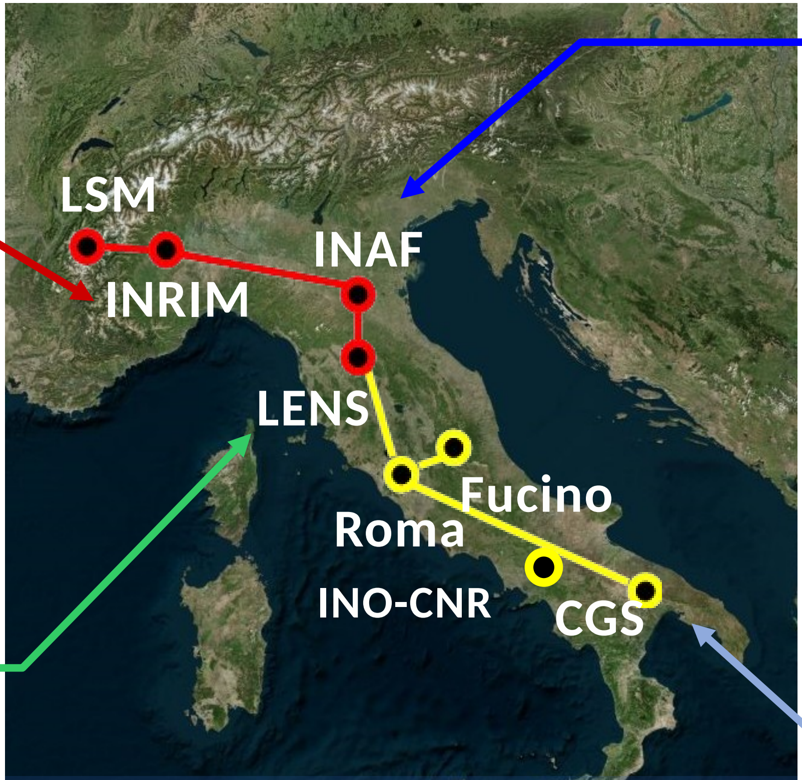


- ✓ **Total Fiber Haul 3000 km**
- ✓ **Two Commercial Dark Fibers available /DWDM and CWDM channels/bidirectional Erbium Doped Fiber Amplifier**
- ✓ **Fiber provided by Consortium GARR and**

## Bologna

32-m dish for Very Long Baseline Interferometry (VLBI)
Part of the Eur
VLBI Network

INAF

## Matera

agenzia spaziale italiana

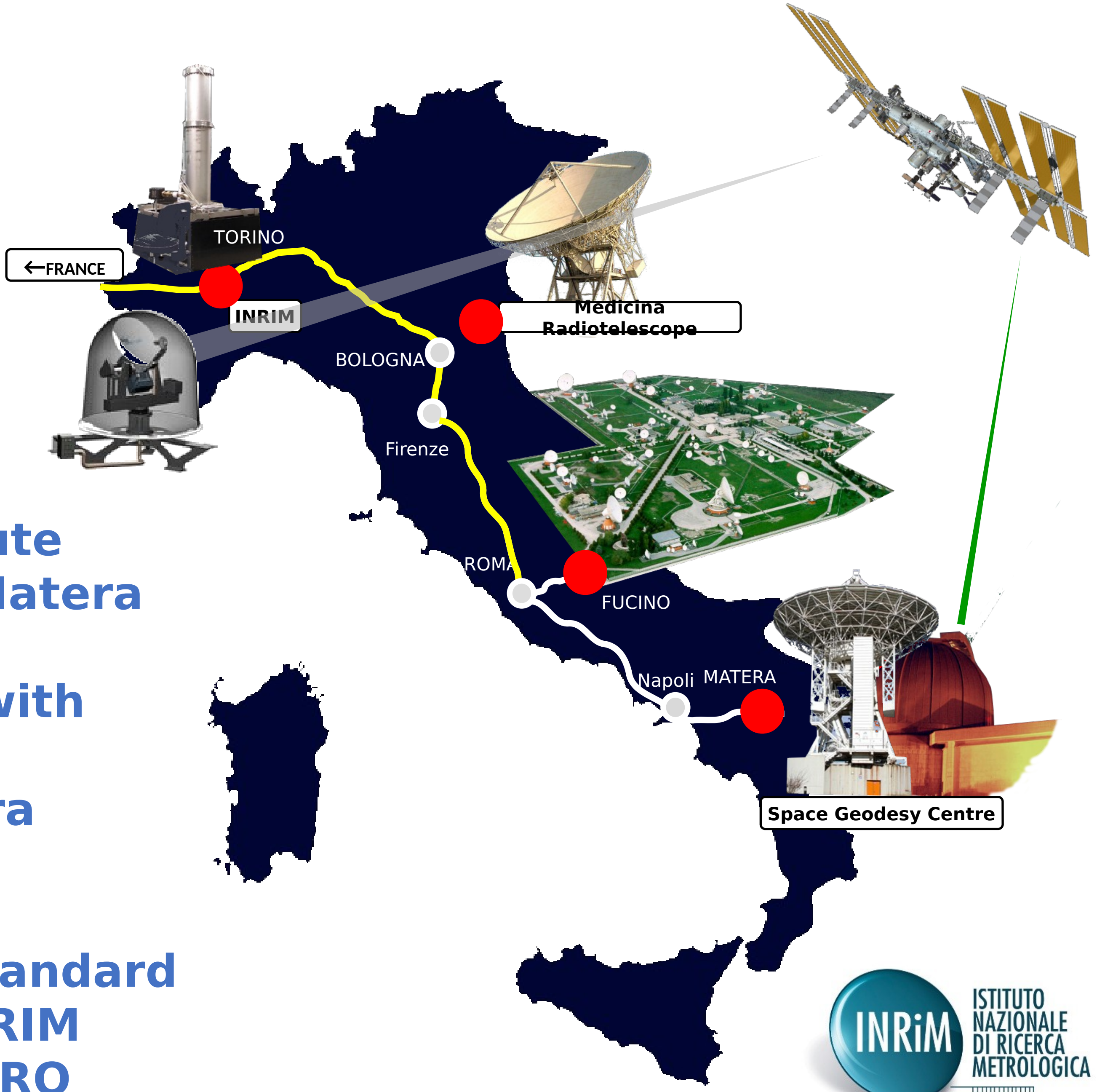


- **H-Maser Absolute calibration in Matera**
- **Geodesy VLBI with common clock Medicina/Matera**
- **Italian Primary Metrological Standard provided by INRIM available at MLRO**

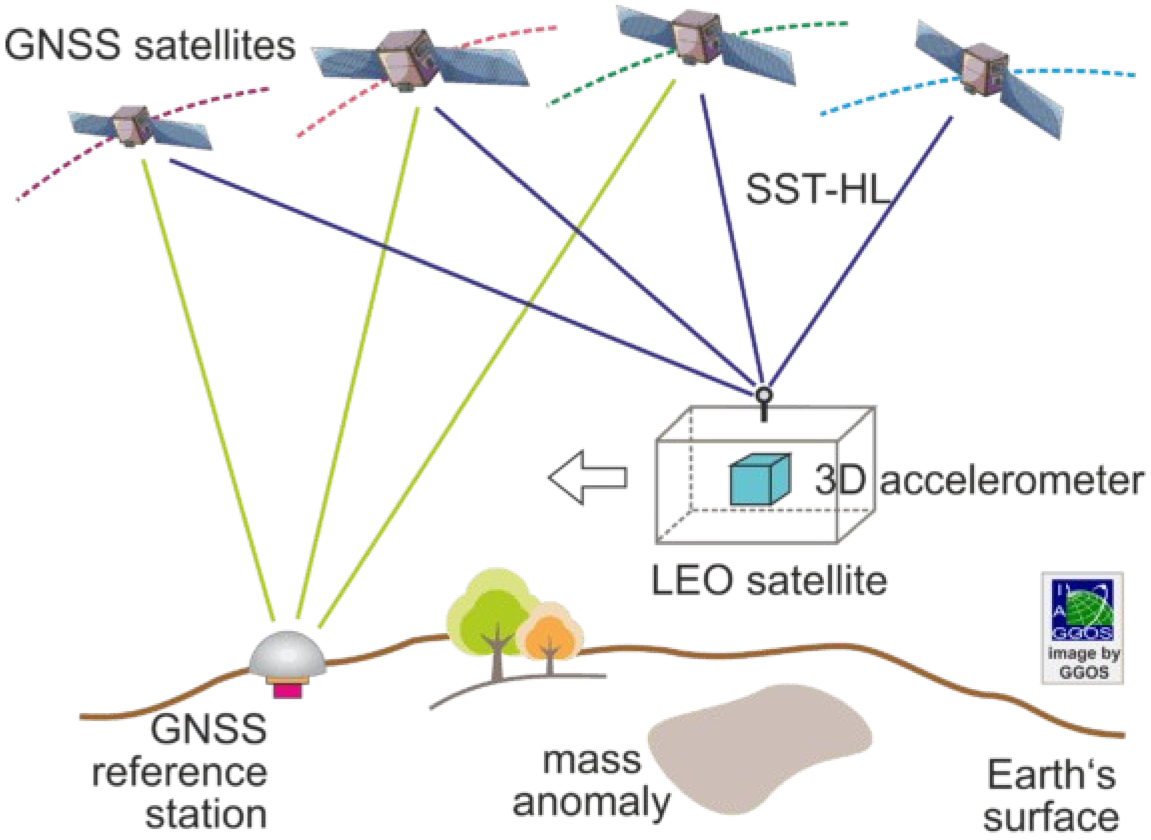


Satellite-to-satellite tracking in the high-low (SST-HL) mode: measurement of accelerations of one low Earth orbiting (LEO) satellite.

The orbit of the satellite is determined using GNSS positioning. The differences with respect to a reference (unperturbed) orbit allow the determination of gravity field at a spatial resolution of 400 km for the static component and about 4,000 km for monthly solutions. The accelerometer records the non-gravitational forces.

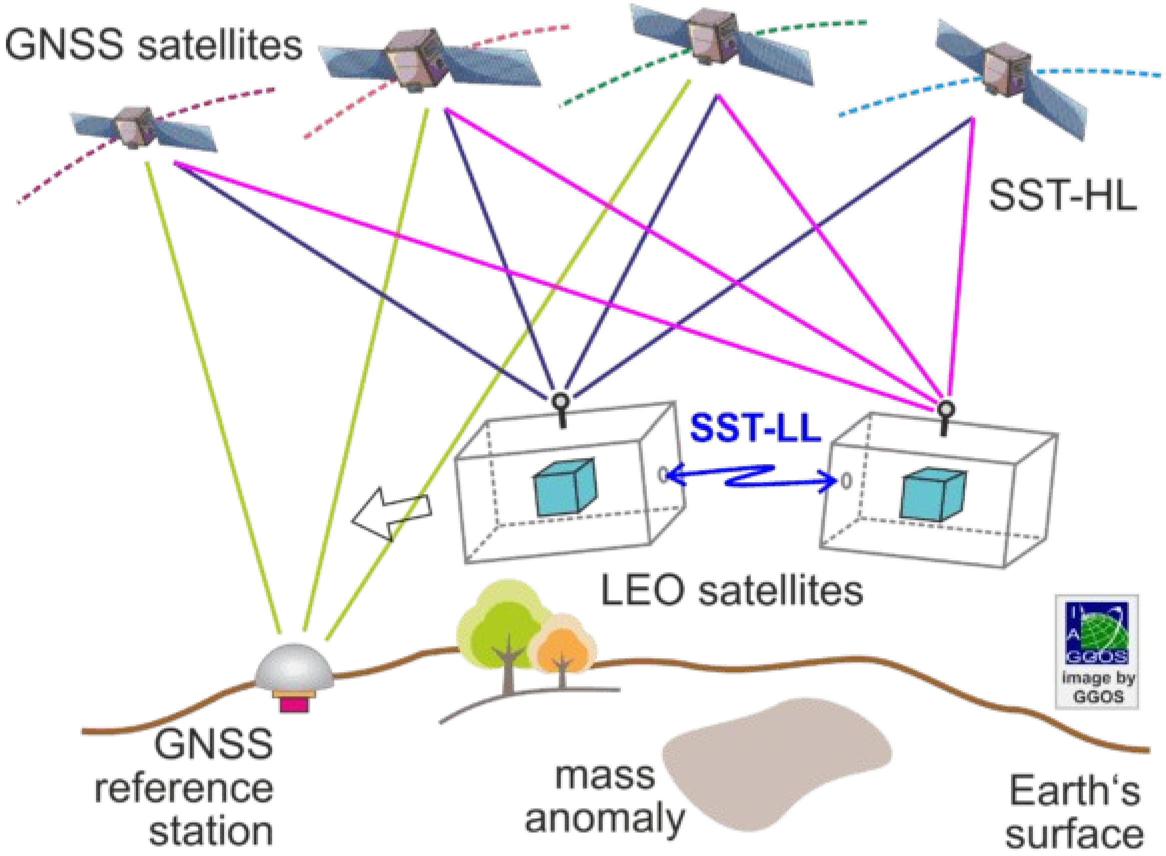


Satellite-to-satellite tracking in the low-low (SST-LL) mode: measurement of acceleration differences between two low Earth orbiting (LEO) satellites.

The orbits of the two satellites are determined using GNSS. The distance between the two satellites is measured with the highest possible accuracy. The acceleration differences between the two satellites allow the determination of the gravity field with a spatial resolution of about 170 km for the static component and about 300 km for monthly solutions.

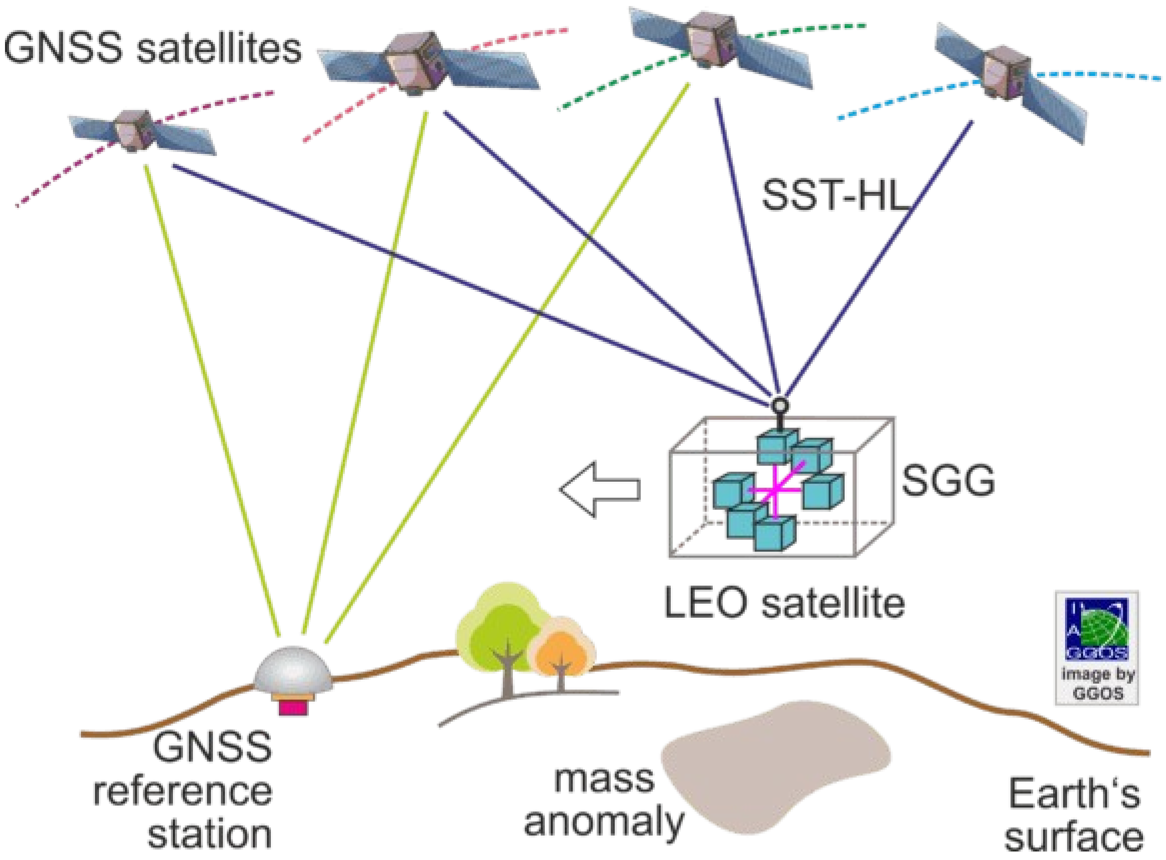


Satellite gravity gradiometry (SGG): in-situ measurement of acceleration gradients within one low Earth orbiting (LEO) satellite.

The satellite orbit is determined using GNSS. The gravity gradients are measured in all three components. This differential measurement allows a spatial resolution of 80 - 100 km for the static gravity field.

# ITRF2020: Preliminary horizontal velocity field

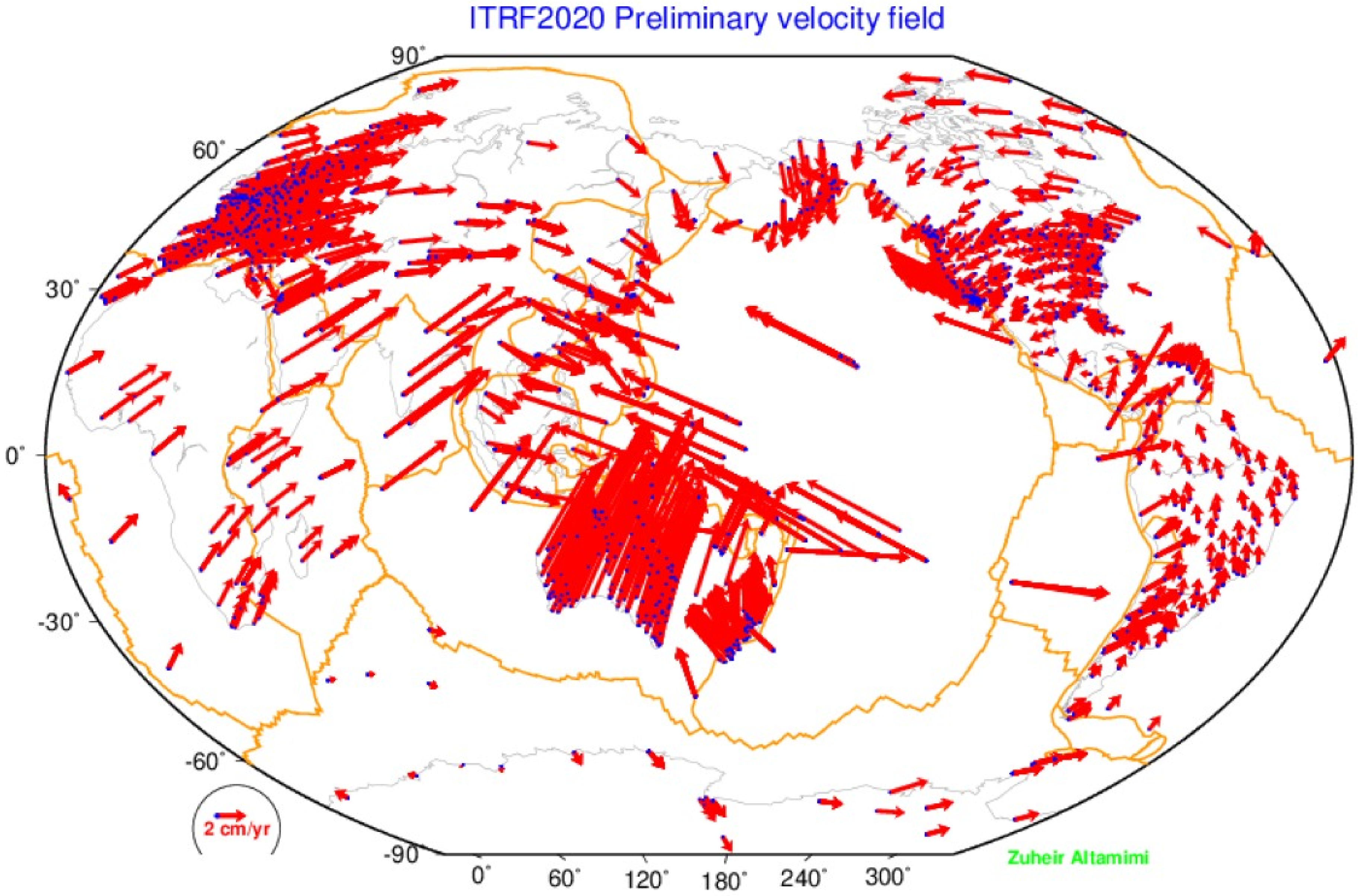

# *ITRF Realization*

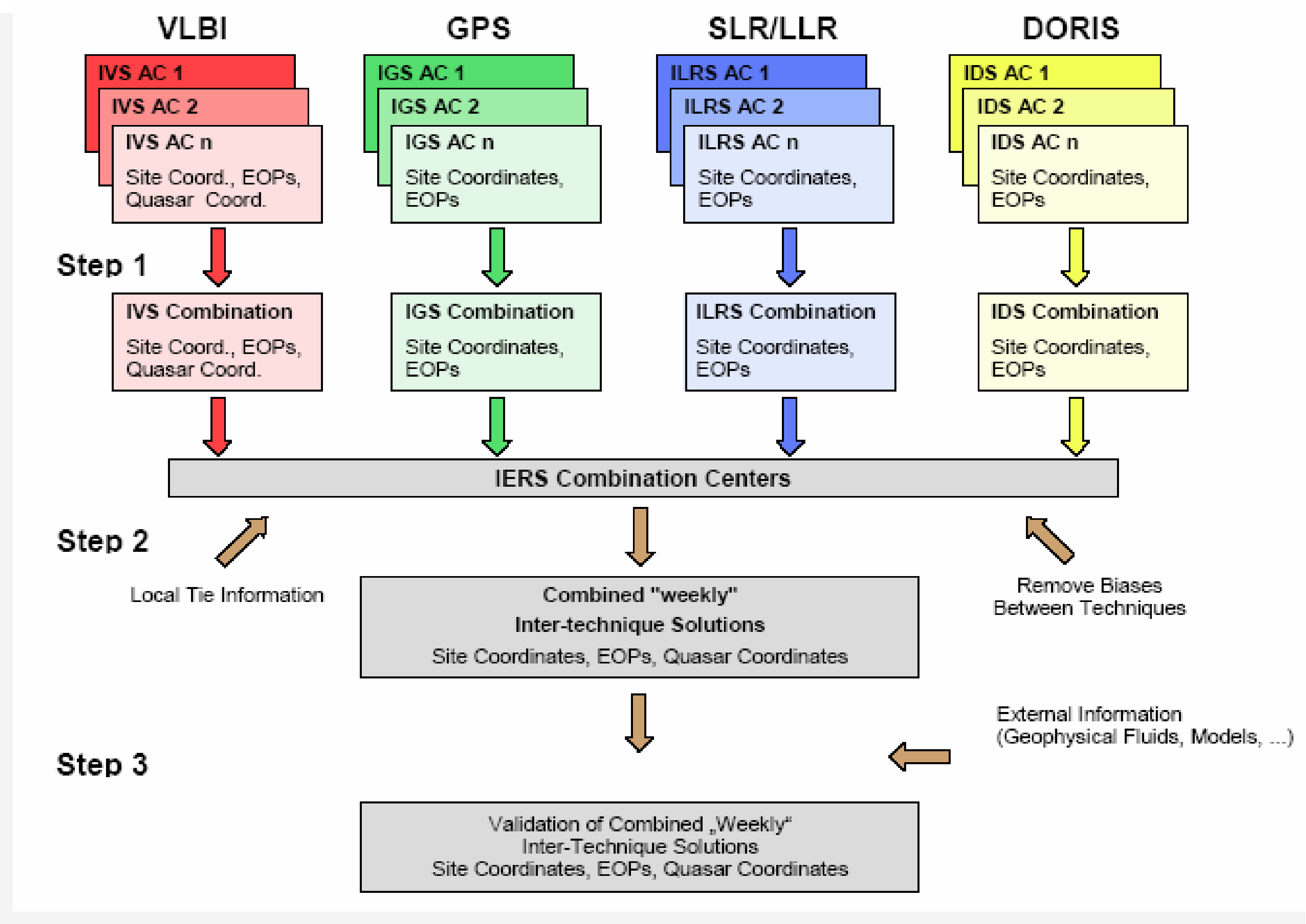


Latest version of the International Terrestrial Reference Frame (ITRF), called **ITRF2020**, published on April 15, 2022.

IGN France is the ITRS Center of the International Earth Rotation and Reference Systems (IERS), in charge of the realization and maintenance of the ITRS

# The ILRS Process Flow for ITRF

- ✓ Time series of weekly SSC and EOP (X, Y and LOD) estimated over 7-day arcs (15-day arcs for the period 1983-1992)
- ✓ SLR data acquired from the global tracking network: LAGEOS, LAGEOS-2, Etalon-1 and Etalon-2
  - data span 1983-2020
  - 1983 to 1992 LAGEOS data only
- ✓ Analysis contributors are generally free to follow their own computation model and/or analysis strategy but a set of guidelines has been agreed within the ILRS Analysis Standing C

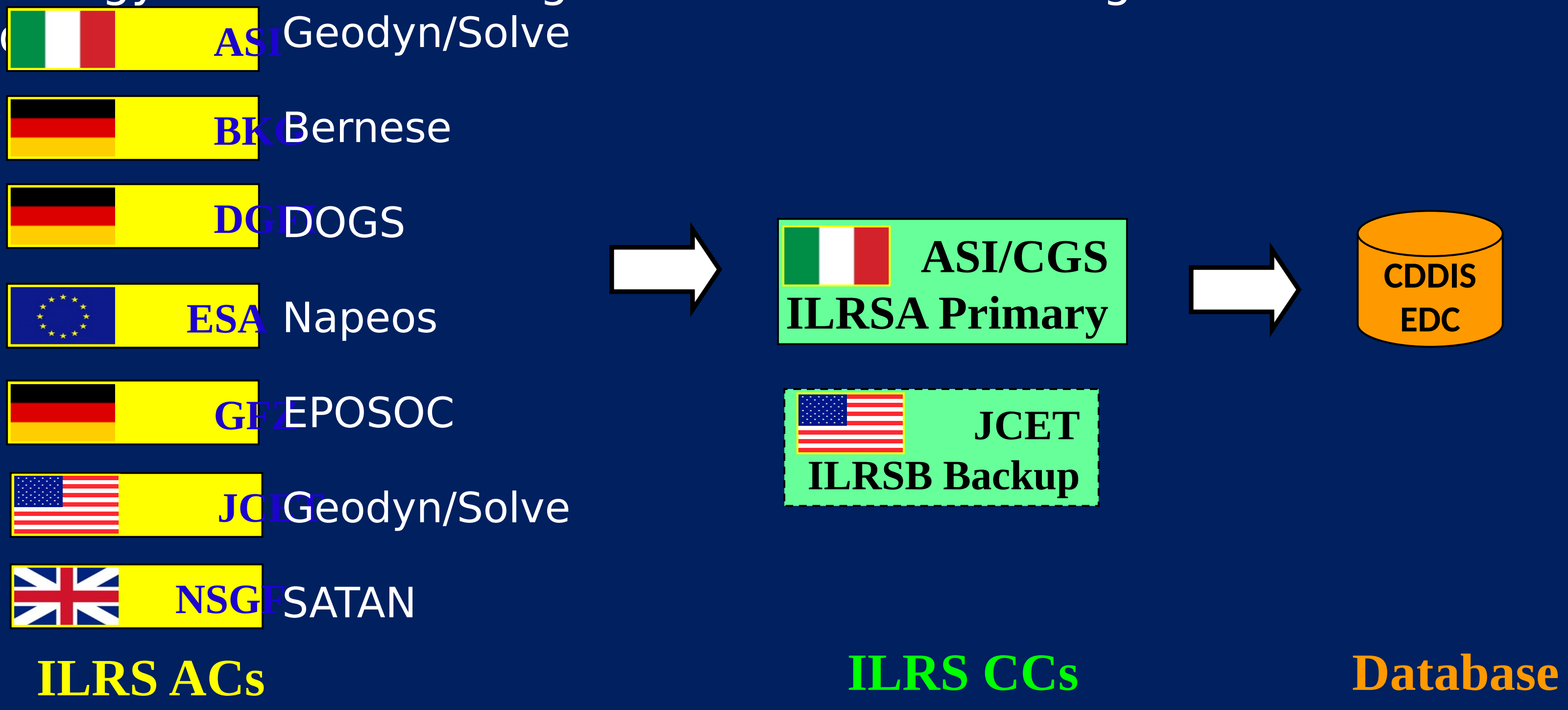

# ITRF2020: Frame definition

**Origin**

- zero translation parameters at epoch 2015.0 and
- zero translation rates

between the ITRF2020 and the ILRS SLR long-term frame over the time-span 1993.0-2021.0

**Scale**

- zero scale and
- zero scale rate

between ITRF2020 and the scale and scale rate averages of VLBI selected sessions up to 2013.75 and SLR weekly solutions covering the time-span 1997.7 – 2021.0.

**Orientation**

- zero rotation parameters at epoch 2015.0 and
- zero rotation rates between the ITRF2020 and ITRF2014

# SLR Scale and Geocenter with respect to ITRF2020

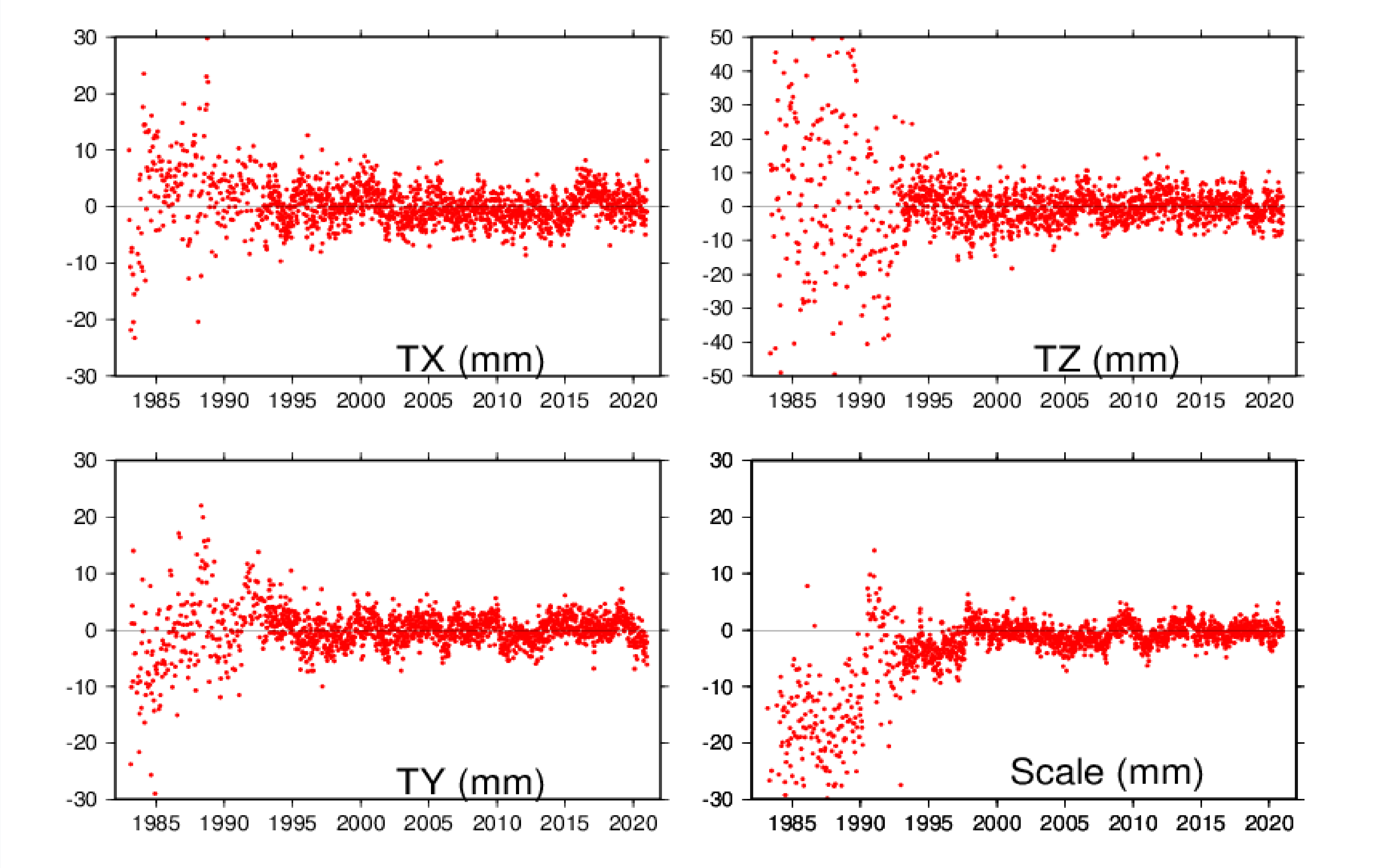


https://itrf.ign.fr/en/solutions/ITRF2020

# Monitoring Geocenter Variations

Mass redistribution within the Earth system affects the position of the geocenter relative to a crust fixed frame.
The geocenter motion is defined as the motion of the center of mass of the Earth (CM) with respect to the geometric center of figure (CF) of the solid Earth surface.

The geocenter motion using SLR data can be estimated using :

## Dynamic method

from degree one unnormalized Stokes coefficients

$$\Delta X(t) = R_e * C_{1,1}(t)$$
$$\Delta Y(t) = R_e * S_{1,1}(t)$$
$$\Delta Z(t) = R_e * C_{1,0}(t)$$

where $R_e$ is the mean terrestrial radius

## Geometric method

as cartesian coordinate offsets from ITRF

$$\begin{pmatrix} X_{ITRF} \\ Y_{ITRF} \\ Z_{ITRF} \end{pmatrix} = \begin{pmatrix} \Delta X \\ \Delta Y \\ \Delta Z \end{pmatrix} + \begin{pmatrix} 1+d & -R_z & R_y \\ R_z & 1+d & -R_x \\ -R_y & R_x & 1+d \end{pmatrix} \begin{pmatrix} X \\ Y \\ Z \end{pmatrix}$$

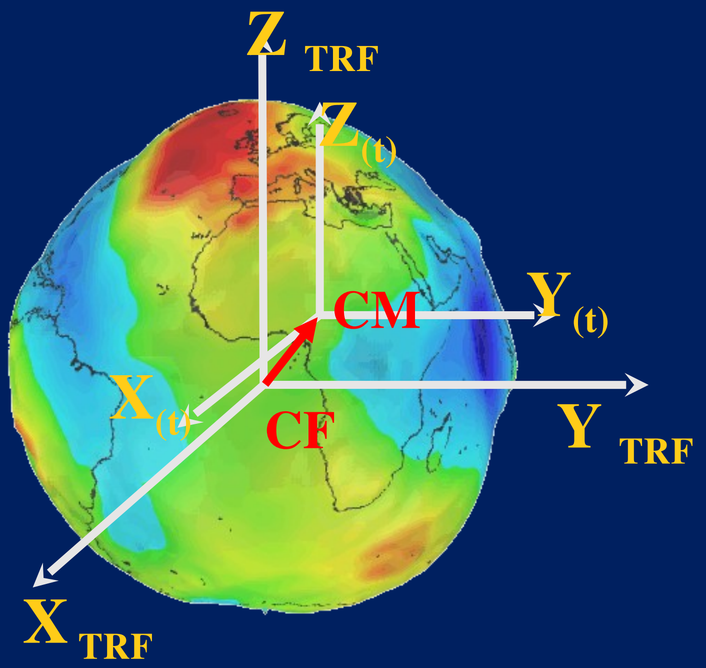

# CM with respect to ITRF2020

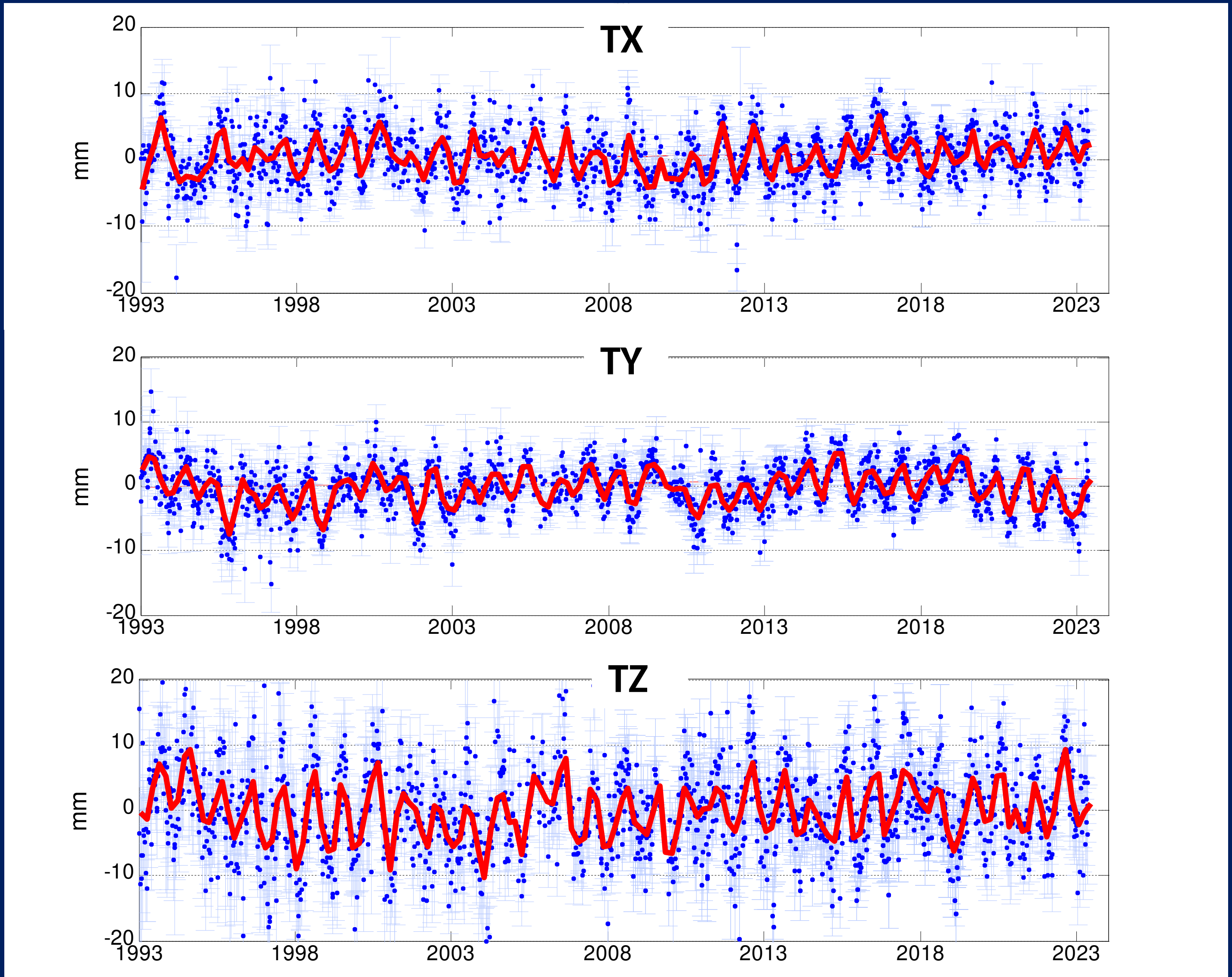


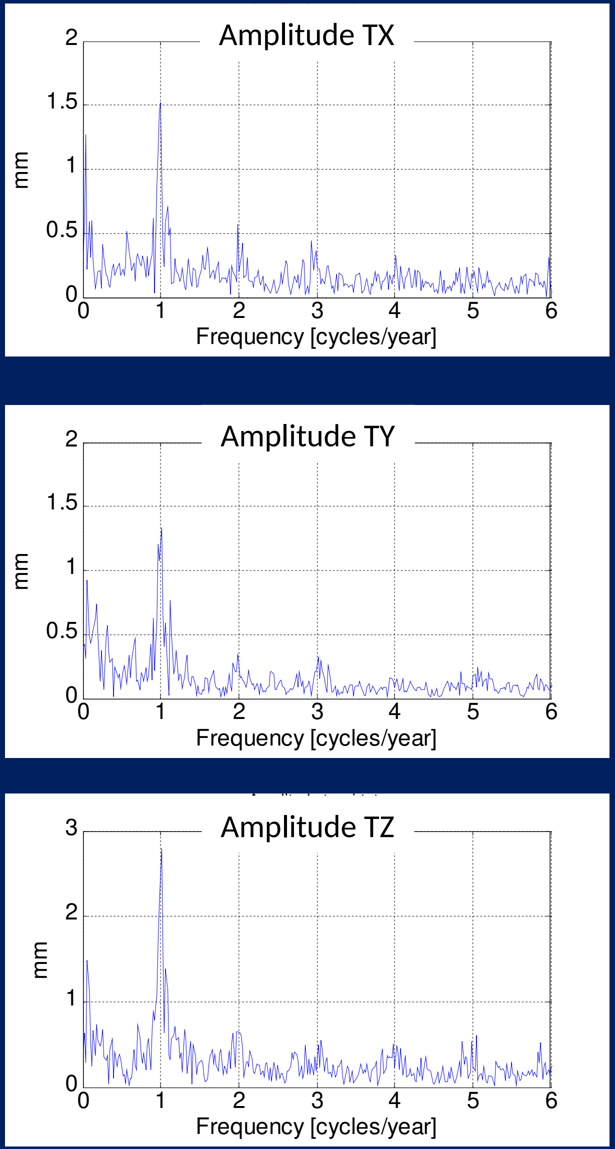

# The geocenter positions in ITRF2020

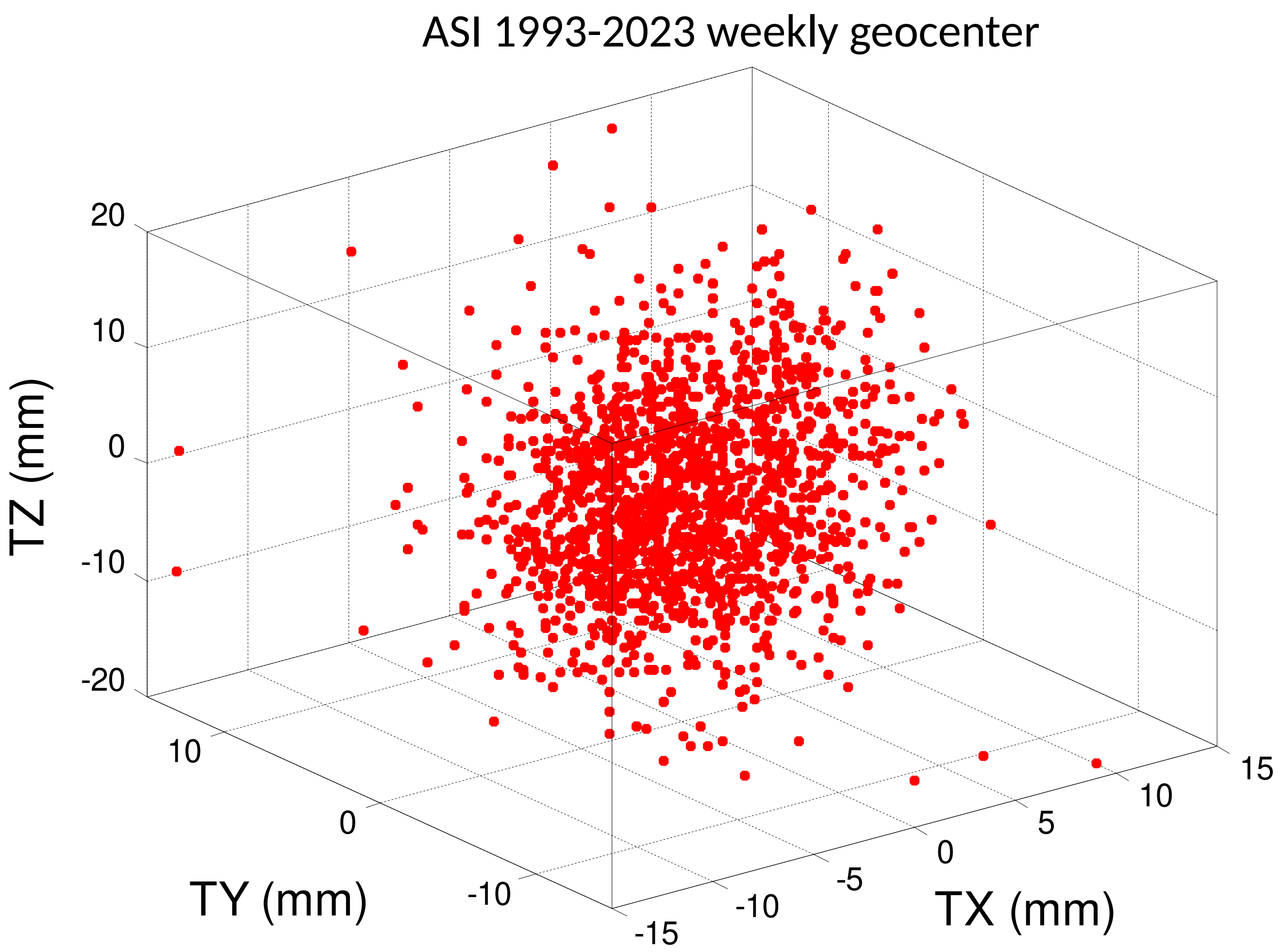


# Polar motion

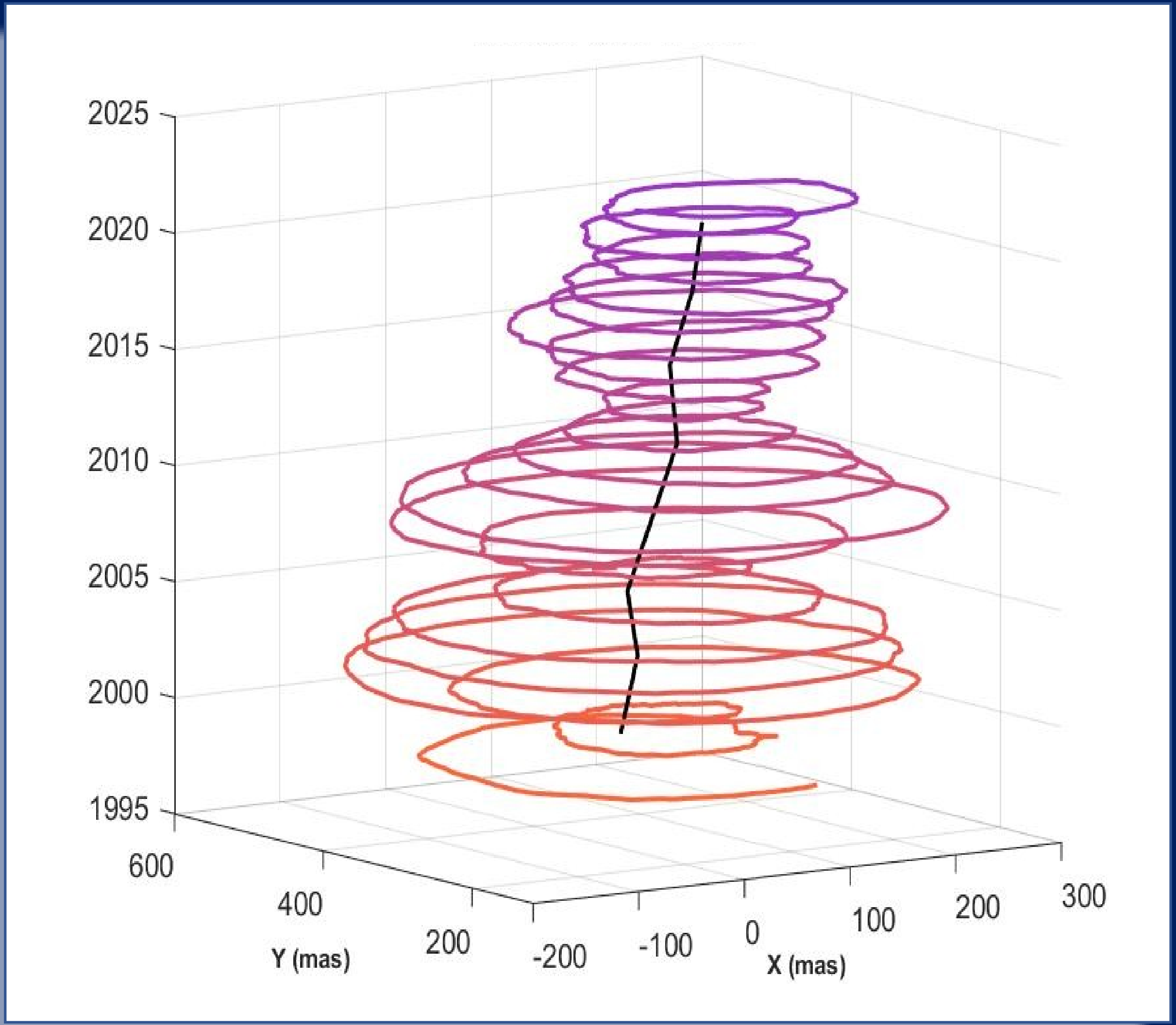


- The polar motion is the motion of the rotation axis of the Earth relative to the crust.
  It has two major components :
  (i) a free oscillation with period about 435 days (Chandler wobble)
  (ii) an annual oscillation

- The Earth Orientation Center of the IERS is in charge of the combined EOPC04 series resulting from a combination of operational EOP series, each of them associated with a given geodetic technique

- The most important mechanism exciting the Chandler wobble is found to be ocean bottom pressure variations (Gross, 2000)

# Polar motion

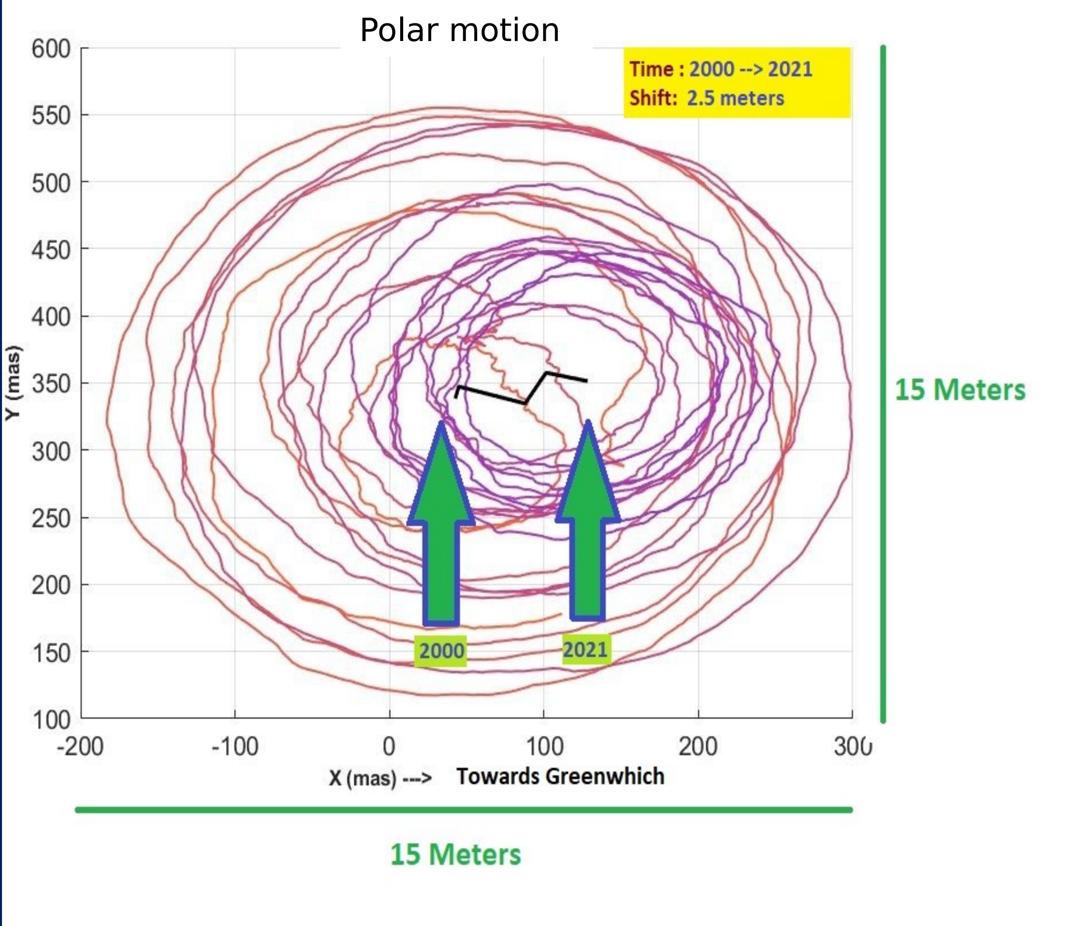


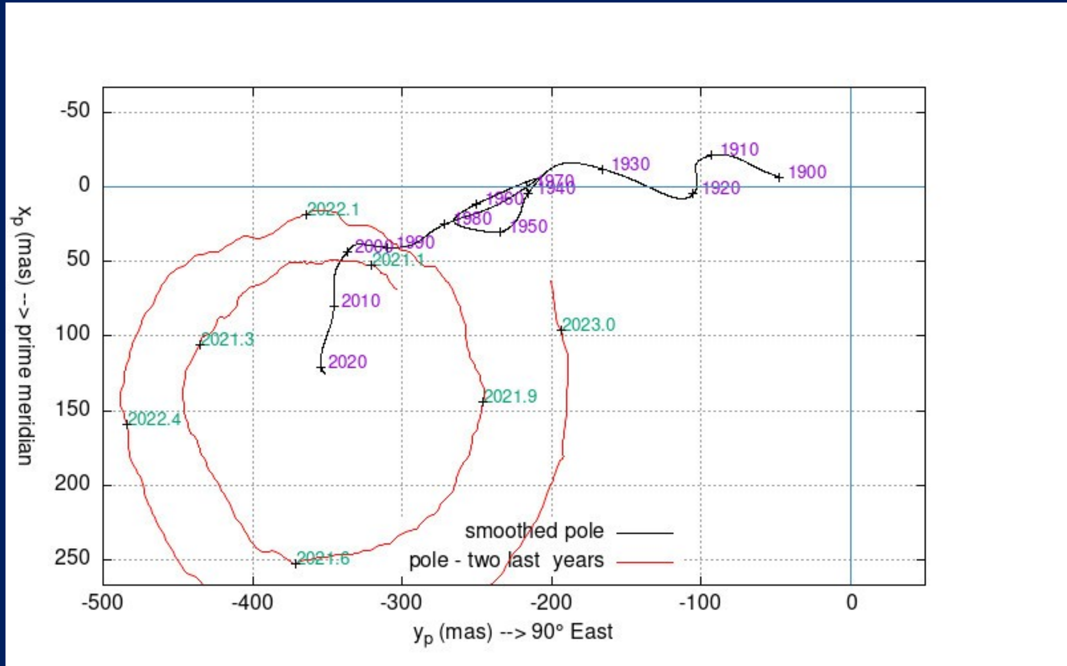


https://hpiers.obspm.fr/

The polar motion considered at time scale larger that 10 year, namely the low-frequency pole, has an irregular drift in in the direction to 80 deg West

The slow drift, about 20 m since 1900, is partly due to motions in the Earth's core and mantle, and partly to the redistribution of water mass as the Greenland ice sheet melts, and to isostatic rebound

# Length of Day

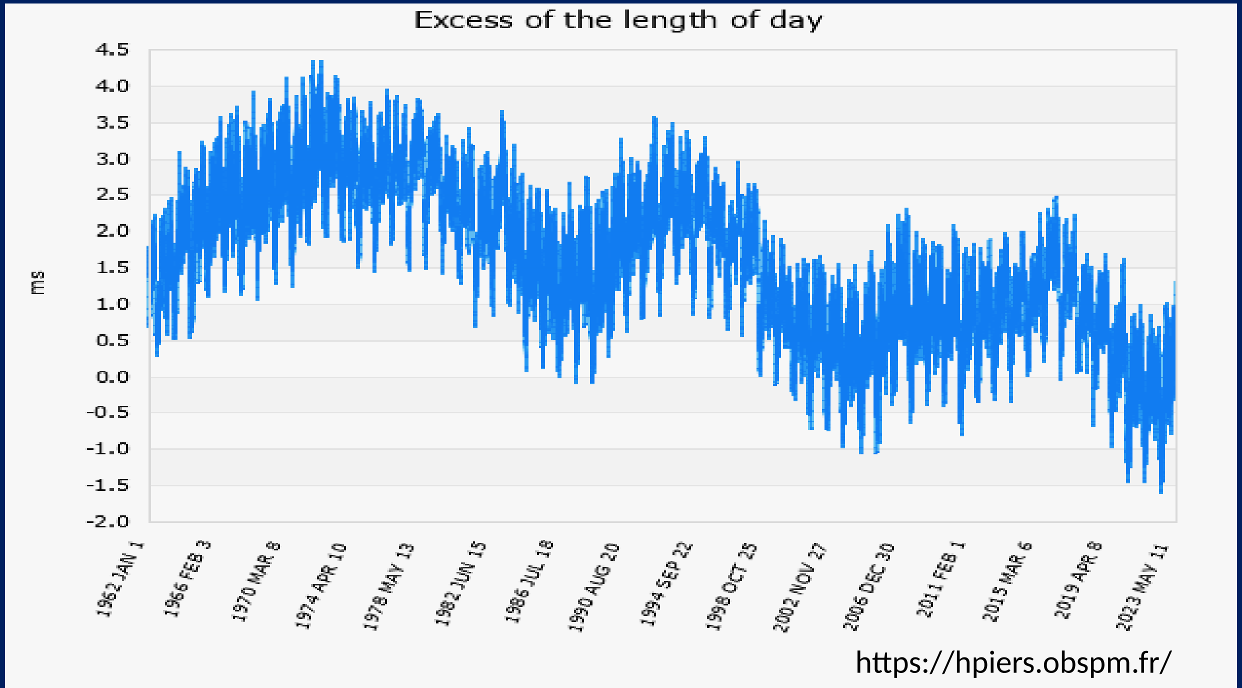


- Improved estimates after 1980 wit the use of space geodetic techniques
- Seasonal and annual variations mainly due to changes in the atmosphere
- Decadal and longer-term variations due to core-mantle coupling
- a secular prolongation of the day by about 1.8 ms in 100 years due to tidal friction and long-term mass variations (*)

From: «Measurement of the Earth's rotation: 720 BC to AD 2015», (F. R. Stephenson et al. 2016)

# The Earth Gravity field

The non-rotating part of the geopotential is represented as a series expansion into spherical harmonics

$$V = -\frac{GM}{r}\sum_{n=0}^{\infty}\left(\frac{a}{r}\right)^{n}\sum_{m=0}^{n} P_{nm}(\cos\theta)\left[C_{nm}\cos(m\lambda) + S_{nm}\sin(m\lambda)\right]$$

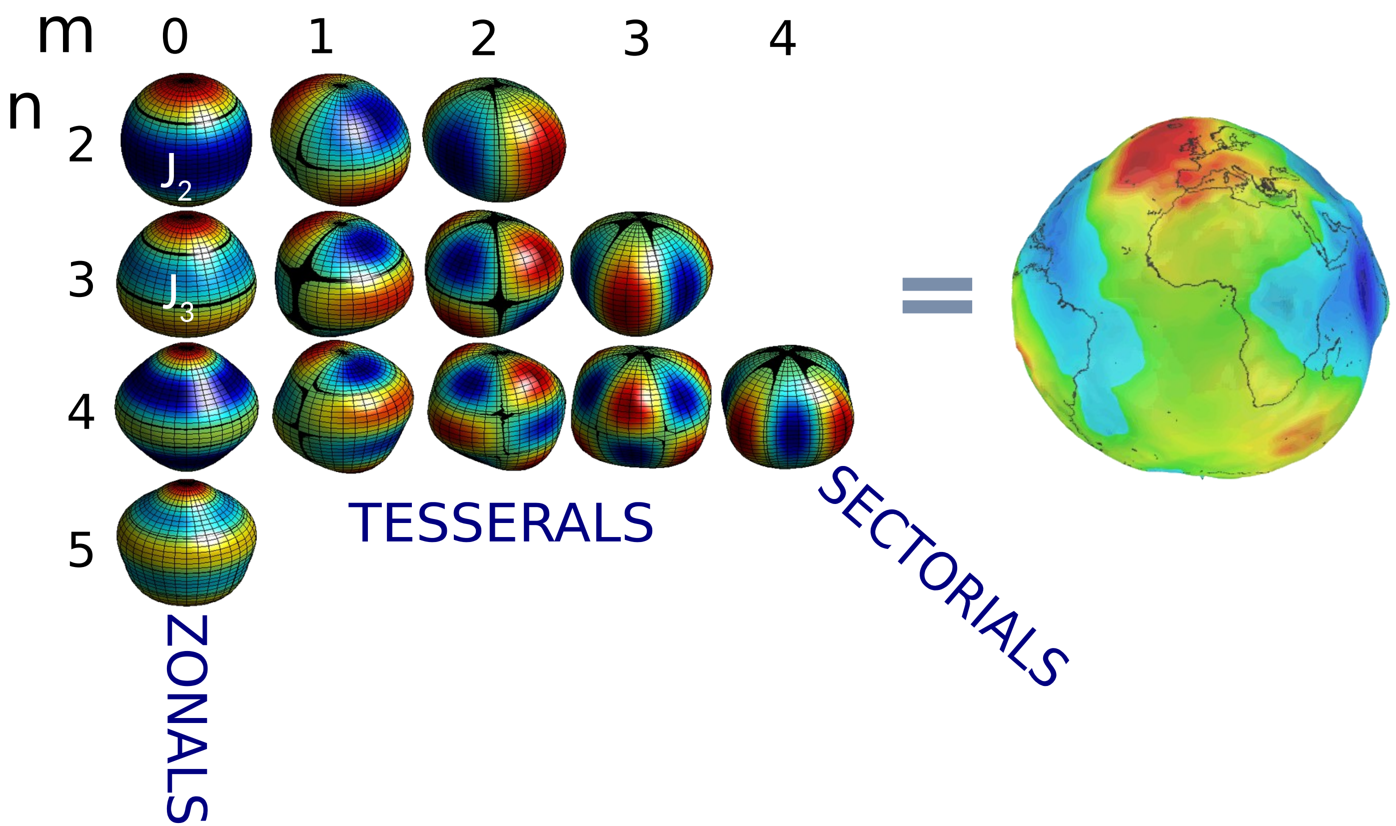

# J2 Time Series from SLR data

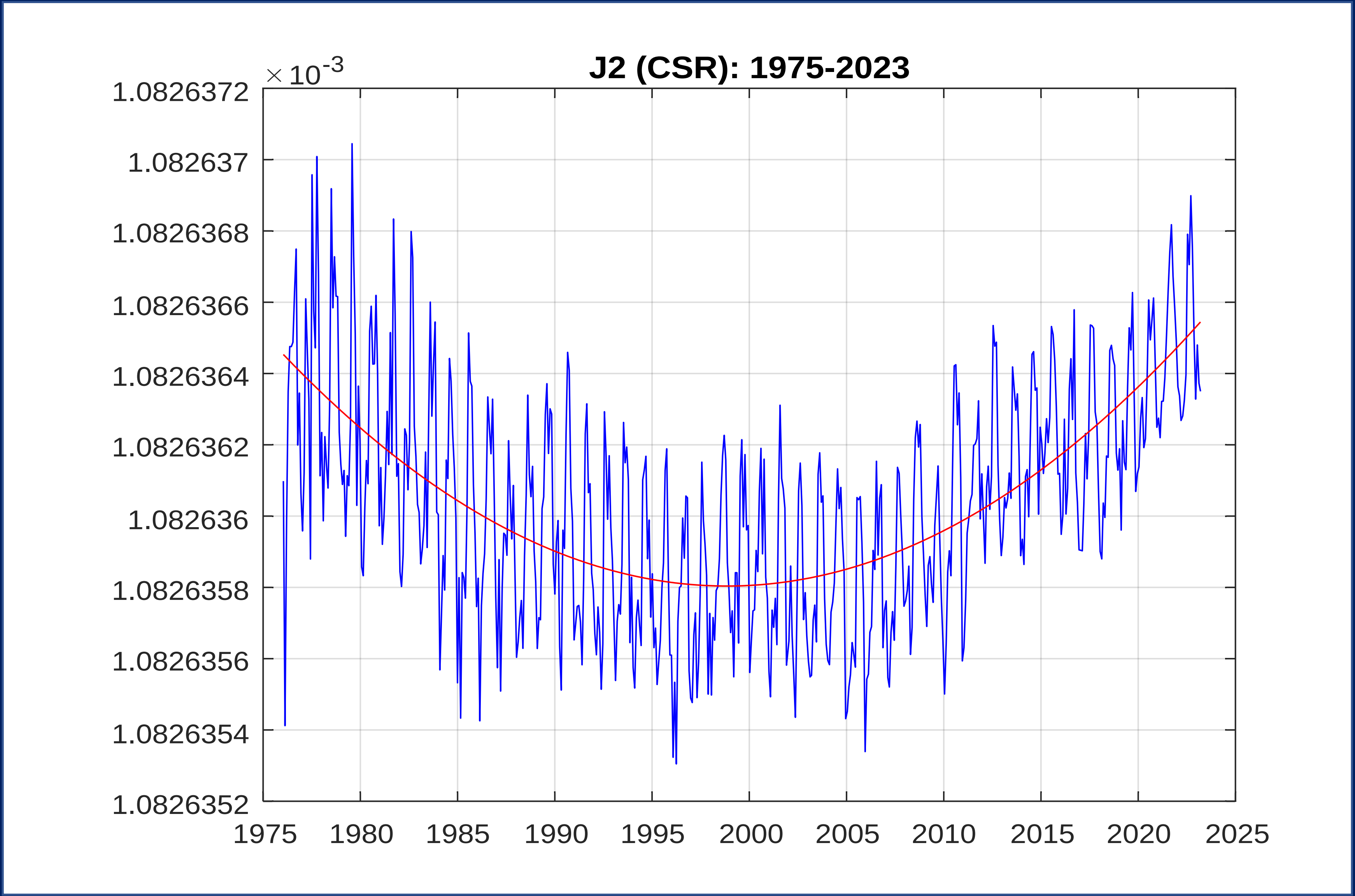


Satellite Constellation:
LAGEOS-1 and 2,
Etalon-1 and 2,
Starlette,
Stella,
Ajisai and
BEC

Cheng, M., B. D. Tapley, and J. C. Ries (2013), "Deceleration in the Earth's oblateness", J. Geophys. Res., doi:10.1002/jgrb.50058.

# $\Delta C_{2,1}$ and $\Delta S_{2,1}$ estimates

The Earth figure axis is the axis of maximun inertia and is represented by the coefficients C21 and S21 of the geopotential

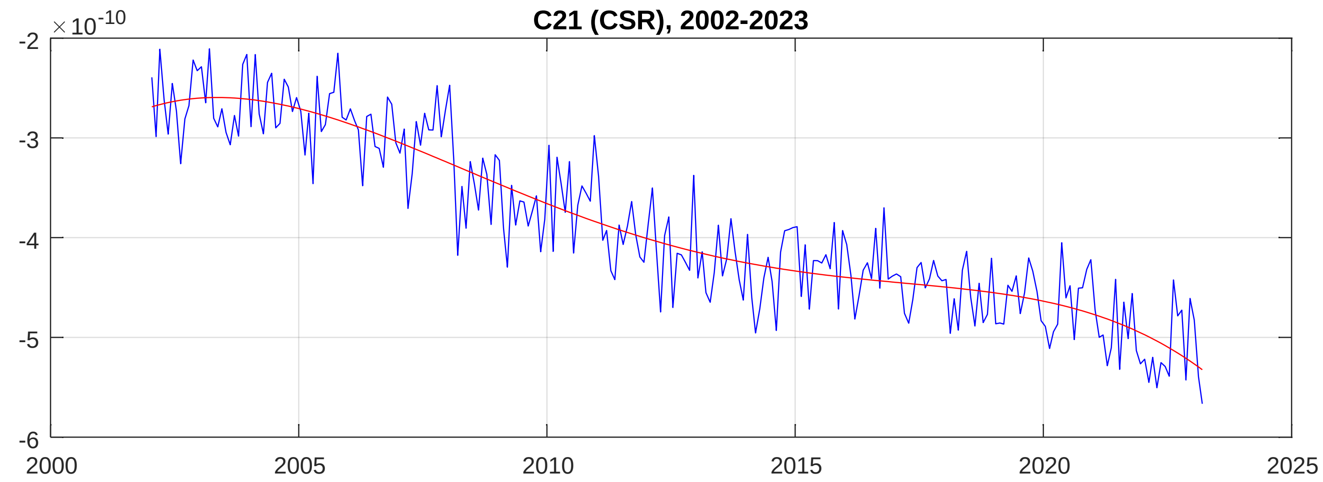


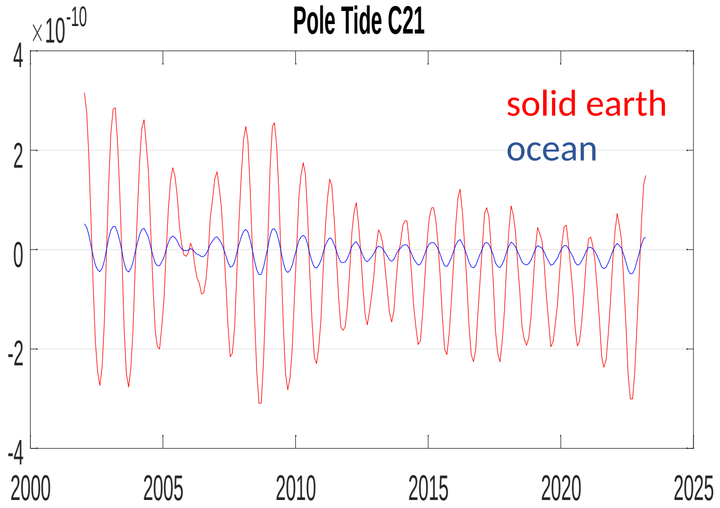


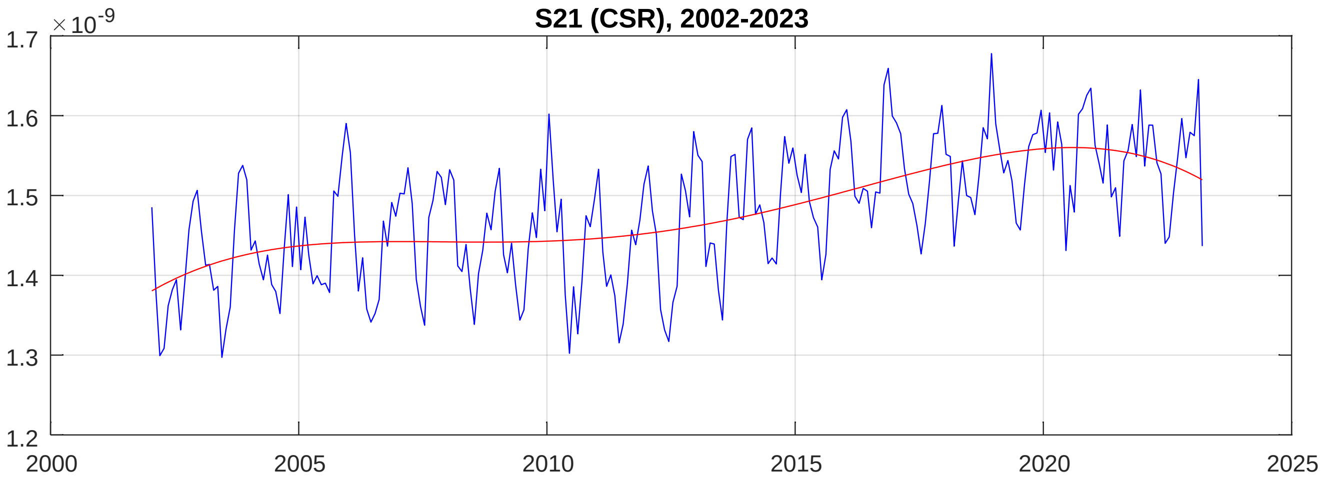


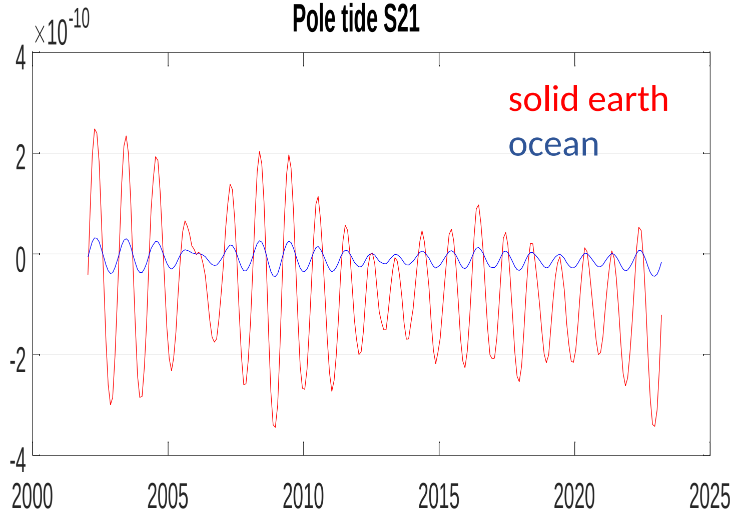

# J3 Time Series from SLR data

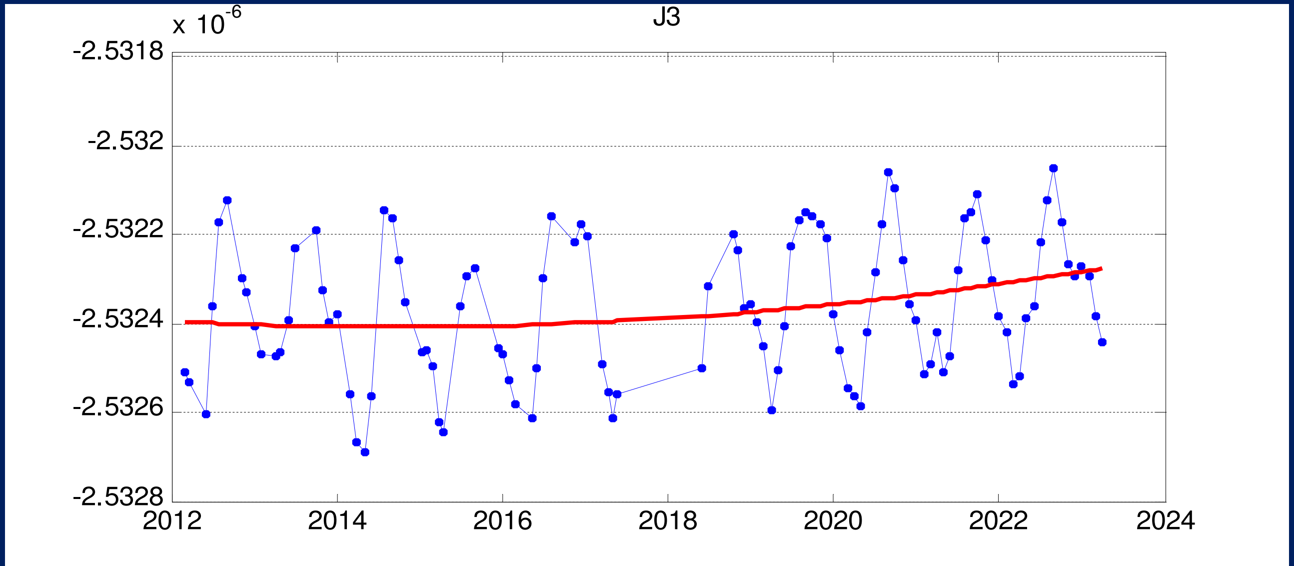


NASA GSFC SLR C20 and C30 solutions
LAGEOS-1/2, Stella, Starlette, AJISAI, Larets, LARES
LARES (launch date 2012) contribution vital due to its combination of low area-to-mass ratio, low altitude, and unique inclination of 69.5°

Loomis et al., 2020, Geophys. Res. Lett., https://doi.org/10.1029/2019GL085488

# THANK YOU